



SPE-XXXXXX-PA

Water Coning, Water and CO₂ Injection in Heavy Oil Fractured Reservoirs

Joachim Moortgat, SPE, School of Earth Sciences, the Ohio State University, Columbus, OH, and Abbas Firoozabadi, SPE, Reservoir Engineering Research Institute, Palo Alto, CA

Copyright 2014, Society of Petroleum Engineers

Abstract

In this work, we investigate challenges related to the recovery of heavy viscous oil from reservoirs with a dense network of fractures and vugs but with a tight matrix. Gravitational drainage of oil from the tight matrix through water injection is ineffective due to the high oil viscosity and density. To further complicate matters, we consider a strong underlying aquifer and there is considerable risk of water coning around producing well bores due to the low water viscosity. To model potential recovery strategies, we carry out simulations with our higher-order finite element (FE) compositional multiphase flow reservoir simulator. Discrete fractures are represented through the cross-flow equilibrium approach. Phase behavior is modeled through equation-of-state (EOS) based phase split computations using the cubic-plus-association (CPA) EOS. Fickian diffusion, facilitating species exchange between gas in fractures and matrix oil, is modeled through chemical potential gradients. First, we validate our simulator by modeling a set of laboratory experiments in which water is injected in a fractured stack saturated with oil. The experiments investigate the effects of capillary pressure and injection rates on oil recovery, and show that at low injection rates capillary imbibition of water from the fractures into the matrix blocks is extremely efficient. Simulations with our 3D discrete fracture model show excellent agreement with the experimental results without parameter adjustments. Next, we consider the detrimental effect of water coning when oil is produced without injection by carrying out a parameter study investigating the impacts of different 1) water-oil mobility ratios, 2) matrix and fracture wettabilities, 3) matrix permeabilities, 4) domain sizes, 5) production rates, 6) well types and placement, and 7) a local viscosity reduction treatment around producing well-bores. We find that the only approach to partially mitigate coning is to produce at low rates from perforated (and potentially multilateral) horizontal wells. As an alternative production strategy, we then model CO₂ injection in 2D and 3D and compare to results from a commercial dual-porosity simulator. CO₂ has a high solubility in this oil and dissolution leads to volume swelling and a large reduction in oil viscosity. In combination with the much higher density difference between the phases, the latter improves gravitational drainage. We find that a significant amount of matrix oil can be produced in addition to oil from fractures and vugs, and with a lower risk of water coning.

Introduction

When oil with a viscosity significantly higher than that of water is produced from densely fractured reservoirs with an underlying aquifer, such as the carbonate reservoirs in some off-shore fields, there is an inherent risk of water coning (Beveridge et al., 1970; Pérez-

Martínez et al., 2012). Coning is a viscous flow instability due to the high adverse mobility ratio between oil and water in the aquifer (Jiang and Butler, 1998; Saffman and G.I., 1958; Tan and Homsy, 1986). Oil production creates pressure gradients throughout the reservoir that drive flow. At the water-oil contact, two-phase flow favors water due to its higher mobility. A dense network of connected fractures provides a pathway for water to the producers, which can result in early breakthrough and poor oil recovery. A similar coning problem can occur from a low viscosity gas cap (Singhal, 1996). The severity of the coning, as for viscous fingering, depends on 1) the production rate (Abass and Bass, 1988; Giger, 1989), which determines the pressure gradients, 2) the viscosity contrast between the two phases (water-oil or gas-oil), and 3) the density difference, which determines the stabilizing gravitational drainage of denser water (Muskat and Wyckoff, 1935). For fractured reservoirs, the propagation of the coning front further depends on the petrophysical properties, such as the fracture density, fracture and matrix permeabilities, fracture-matrix porosity partitioning, and the wettability of the rock, which determines capillary imbibition of water from the fractures into the matrix. Finally, the impact of coning on oil recovery is affected by production strategy (in additional to rate). The time of breakthrough is determined by the distance of the wells from the water-oil (or gas-oil) contact, and pressure gradients are influenced by the type of wells, i.e. vertical or (multilateral) horizontal wells. Operational constraints also determine the amount of water production that can be handled by surface facilities. Most off-shore oil fields, in Mexico for instance, currently lack such facilities (Pérez-Martínez et al., 2012). Significant water production due to coning requires wells to be shut-in prematurely. Below a certain critical production rate (Schols, 1972), viscous forces are balanced by gravity and coning can be prevented, but for densely fractured reservoirs the subcritical production rates may be too low to be economically viable.

Due to the potentially disastrous impact of water coning on oil production, there is considerable interest in better modeling capabilities of coning in fractured media, which is considered one of the most challenging problems in reservoir engineering. Early theoretical (Muskat and Wyckoff, 1935; Chaney et al., 1956; Schols, 1972; Giger, 1989) as well as numerical studies (Beveridge et al., 1970; Letkeman and Ridings, 1970; Settari and Aziz, 1974) have been carried out in the distant past. More recent studies of water coning in fractured media have relied on the dual-porosity and dual-permeability models (Warren and Root, 1963; Firoozabadi and Thomas, 1990; Pérez-Martínez et al., 2012). It is well known, however, that dual-porosity models, while computationally efficient, compromise in the representation of the relevant physics, especially for complicated multiphase problems. Fractures and matrix blocks are modeled on two dual grids and all interactions between the fractures and the matrix have to be described by semi-empirical transfer functions, which may not be rigorous. Gravitational reinfiltration, capillary effects, phase behavior in compositional multiphase flow, Fickian diffusion, and general configurations of fractures are difficult to reconcile with the dual-porosity framework (though modifications have been proposed to improve on several of these limitations).

In this work, we study coning with a *discrete* fracture model that explicitly takes into account all convective, capillary, gravitational, and diffusive fluxes between the fractures and the matrix. To the best of our knowledge, coning has not been studied in the context of discrete fracture models before, and doing so provides new insights in the process that may not have been captured by earlier studies.

In our model, discrete fractures are combined with a small neighborhood of the matrix blocks into larger computational elements. The assumption is that the fluid in the fractures instantaneously equilibrates (mixes) with the fluid immediately next to it in the matrix due to a high transverse matrix-fracture flux (which does not need to be explicitly calculated). This assumption is referred to as the cross-flow-equilibrium (CFE) approach and the computational elements that contain both the fracture and some matrix fluid are CFE

elements. The flux across the edges between two CFE grid cells properly integrate over the fracture aperture and width of the matrix slice, taking into account different relative permeabilities in the fracture and matrix. For example, the matrix part of the CFE may have a high residual oil saturation, while the fracture part may not have residual oil. In the direction orthogonal to the fractures, the flux between a CFE element and a matrix element is equivalent to that between two matrix elements. This approach was first applied to single-phase (Hoteit and Firoozabadi, 2005) and two-phase (Hoteit and Firoozabadi, 2006) compressible and compositional flow without capillarity in 2D fractured domains, and more recently to three-phase compositional flow in 3D domains with capillarity (Moortgat and Firoozabadi, 2013c,b,a). Alternative discrete fracture models have been proposed for black oil (Geiger et al., 2009) and immiscible incompressible flow (Hoteit and Firoozabadi, 2008).

In this work, we first demonstrate the accuracy and reliability of our discrete fracture model by simulating a set of experiments in which water was injected in a fractured stack saturated with oil (Pooladi-Darvish and Firoozabadi, 2000). Capillary imbibition between the fractures and the water-wet matrix is studied as a function of injection rate. The same experiment was modeled before using a control volume finite difference method (Monteagudo and Firoozabadi, 2007).

Our studies of water coning and CO₂ injection consider vuggy reservoirs with a triple porosity of matrix, vugs, and fractures. In our representation of such domains, we divide the triple porosity into CFE elements that contain both the fractures and the connected vugs, and matrix elements that contain the tight matrix and unconnected vugs. A large fraction of the oil may reside in the fractures and vugs, which makes the CFE approach particularly suitable. Similar conditions were investigated before in a dual-porosity framework (Pérez-Martínez et al., 2012).

To model compressible and compositional multiphase flow, we use a higher-order discontinuous Galerkin (DG) method for the transport equations, which updates the molar density of each fluid component. The flow equations are solved by a mixed hybrid finite element (MHFE) method, which simultaneously solves for globally continuous velocity and pressure fields, both to the same order accuracy. An accurate velocity field in heterogeneous and fractured domains is the main strength of the MHFE approach. More generally, the combination of the DG and MHFE higher-order finite element methods is a considerable improvement over lowest order finite difference and finite volume methods, particularly for fractured reservoirs. A detailed description of these methods and comparisons to other approaches are given in our earlier work (Moortgat and Firoozabadi, 2010; Moortgat et al., 2012; Moortgat and Firoozabadi, 2013a,b,c).

After demonstrating that early water coning is likely to occur in densely fractured carbonate reservoirs with an underlying aquifer, we investigate CO₂ injection as an alternative production strategy for the same reservoir conditions, but with an even denser fracture network. During CO₂ injection, the fractures provide a large interaction surface through which Fickian diffusion can occur, driving species exchange between the fractures and the matrix, thereby delaying breakthrough of injected gas. Additionally, mixing of CO₂ with the dense viscous oil in this reservoir results in advantageous phase behavior. CO₂ has a 75% solubility in this oil, which can lead to 40% swelling of the oil volume (expelling it from the matrix), and a 25-fold reduction in the oil viscosity, which improves gravitational drainage of oil from the matrix into the fractures. The modeling of multi-component multiphase Fickian diffusion is challenging, particularly in fractured domains, where the conventional description in terms of compositional gradients fails. We resolved these issues in a recent work (Moortgat and Firoozabadi, 2013a) by considering gradients in chemical potential as the driving force. The

importance of Fickian diffusion when gas is injected in fractured reservoirs is another example where most reservoir simulators have severe limitations. We show that [an improper treatment of diffusion can result in significantly underestimating](#) the efficient oil recovery from CO₂ injection. [Additionally, we compare our results to a commercial dual-porosity reservoir simulator that uses our model for Fickian diffusion.](#)

The paper is organized as follows. First, we model a set of experiments (Pooladi-Darvish and Firoozabadi, 2000) in which water is injected at different rates into a stack of chalk blocks divided by a number of discrete fractures and investigate the importance of capillary imbibition into the water-wet matrix. The modeling of this complicated experiment demonstrates the reliability of our discrete fracture model in accurately reproducing experimental data. We then proceed to study the risks of water coning when dense and viscous oil is produced from a fractured reservoir that has an underlying aquifer. The third study considers the alternative of CO₂ injection, in which Fickian diffusion and favorable phase behavior lead to considerably higher oil recovery without risk of coning. We end with concluding remarks.

Experiment and Modeling of Water Injection Into a Fractured Stack

Pooladi-Darvish and Firoozabadi (2000) performed a set of experiments in which water was injected [into](#) the bottom of a fractured stack of oil-saturated Kansas chalk blocks. Initially, the stack was saturated with *n*C₁₀ at atmospheric pressure and room temperature (59°F). At these conditions the ‘oil’ density is 0.8 g/cm³ and the viscosity is 0.94 cp, while the water density and viscosity are 0.95 g/cm³ and 1 cp, respectively (note that in this experiment, the flow is viscously stable). The relative permeability and capillary pressure curves in the fracture and matrix are given in **Figure 1** and are chosen the same as in an earlier analysis (Monteagudo and Firoozabadi, 2007). Details are provided in the figure caption. Of particular importance in the discussion below is the residual oil saturation of 35%.

The dimensions of the stack are 19 × 19 × 122 cm³, with vertical fractures on all 4 sides as well as at $x = 6.35$ cm and $x = 12.7$ cm. Horizontal fractures are located at the top and bottom as well as at $z = 30.5$ cm, $z = 61$ cm and $z = 91.5$ cm. These fractures separate 12 matrix blocks with a porosity of 30% and permeability of 2.5 md. The fractures have apertures in the range of 150 – 200 μm. For our numerical modeling, we assume 2 mm cross-flow elements with 1.4×10^6 md permeability ([using the cubic law in terms of the aperture](#)), and we consider 3 levels of grid refinement: Grid 1 (13 × 7 × 41), Grid 2 (13 × 13 × 79), and Grid 3 (7 × 6 × 29). The configuration of the fractures and chalk slabs are illustrated for Grid 2 in **Figure 2**, with 4 boundary fractures omitted for visualization.

In the experiment, water is injected from the bottom at four constant injection rates of 0.26, 0.78, 1.95, and 3.85 pore volume (PV) per day with constant pressure production from the top. Figure 2 shows the water saturation at 40% PV injected (PVI) for all four rates simulated on the finest Grid 2. As expected, we find that propagation of water through the fractures is delayed by capillary imbibition into the matrix blocks, which is most effective for the lowest rates.

The measured and simulated (on all 3 grids) oil recovery factors for all injection rates are given in **Figure 3**. The ultimate oil recoveries at 2 PVI, from lowest to highest injection rates, are 67.5%, 66.8%, 64%, and 63.3%, showing a maximum incremental recovery of 6.6% due to the efficiency of capillary imbibition at lower injection rates. At the lowest injection rate we have essentially piston-like displacement of the non-residual matrix oil: the front propagates at the same rate in the matrix and the fracture, resulting in the sharp cut-off in recovery at the time of water breakthrough. Note that the oil recovery factor is higher than $1 - S_{row} = 65\%$ because

we include the 2.5% of oil initially in the fractures. We emphasize that such high oil recovery from fractured reservoirs due to imbibition does not only occur at the laboratory scale, but also in densely fractured field scale reservoirs (Moortgat and Firoozabadi, 2013b,c).

We can accurately simulate this complex problem of two-phase flow with capillarity in a 3D fractured domain with our CFE discrete fracture model, and the results have essentially converged even on the coarsest grid. In our simulations, no parameters were adjusted in order to match the experimental results. The CPU times for the simulations with our compositional model were 3 hrs on Grid 1, 16 hrs on Grid 2, and 30 min on Grid 3. This compares favorably to modeling of the same experiment on a 1,800 element grid using a control volume finite difference method for an immiscible formulation (Monteagudo and Firoozabadi, 2007), which required 27 hrs of CPU time (on a Pentium PC 2.66 GHz, versus a 2.8 GHz Intel i7 core used in this work). Should we have used an immiscible formulation, our CPU efficiency would have been even higher. Moreover, our CFE model becomes more efficient for large-scale domains where we can allow for wider cross-flow elements than the 2 mm widths used in this example.

This comparison to experimental data gives us confidence in the modeling of larger scale problems considered in the next examples. The more general conclusion from this example is that water-flooding can be highly effective for densely fractured water-wet reservoirs due to capillary imbibition.

Water Coning in Fractured Off-Shore Heavy Oil Reservoir with Underlying Aquifer

We study the effect of coning when oil is produced without injection from a heavy oil reservoir with a strong underlying aquifer. As discussed in the introduction, we consider reservoirs with a complicated triple porosity consisting of tight matrix, a large number of connected and unconnected vugs, and a dense network of fractures. However, while the effective reservoir permeability is known, the details of the fracture network are not. Given this uncertainty, there are several ways that we can set-up our simulations: we can have a large number of fractures with a small aperture, or a smaller number of fractures with a wider aperture. The latter allows coarser grids and more efficient computations. Fracture spacing and matrix block size will affect the fracture-matrix interactions, which will be considered in the examples.

Reservoir Description and Simulation Set-Up The flux through the fractures depends (numerically) on the fracture aperture times the fracture permeability: we can decrease one and increase the other and obtain similar result. Instead of using the cubic law between fracture aperture and permeability, we choose the fracture aperture, fracture spacing, and fracture permeability to agree with a measured effective permeability of around 1 d (based on well testing), and a given fraction of oil in the fractures and the vugs. Specifically, as a base-case we consider 4 m \times 4 m matrix blocks, surrounded by 4 cm fractures with a permeability of 100 d, and 40 cm wide CFE elements that represent both the fractures and connected vugs. The matrix (and unconnected vugs) blocks have a porosity of 8% and permeability of 1 md. With this configuration, the effective permeability in each direction is 1 d, the fraction of oil in the fractures is 20%, and the fraction of oil in the fractures plus the connected vugs is 33%. This high fraction of oil in fractures and vugs in certain off-shore Mexican oil reservoirs is what makes them potentially attractive for hydrocarbon production. As we will see below, very little matrix oil can be recovered through depletion. The recovery from water injection is also known to be low, due to mixed-wetting conditions.

For most of our simulations, we assume a 180 m oil column with a large underlying aquifer. In the horizontal directions, we will

investigate the importance of domain size by considering 52, and 400 m dimensions in these directions, and in the vertical direction we will consider two examples with a 380 m thick reservoir. Because the Darcy-flow in the matrix blocks is slow at best, those are discretized by single grid cells to speed up the computations (discretizing the matrix blocks with multiple grid cells is more critical when capillarity is important, to resolve saturation gradients as in the previous example, or to resolve compositional gradients that drive Fickian diffusion, as in the final example). The aquifer is modeled by the grid cells in the bottom 20 m of the mesh. These elements are given a porosity of 100, which results in a similar pressure gradient at the water-oil contact as having very large (or many) grid cells with the same porosity as elsewhere. By having a large PV of slightly compressible water in the domain, we prevent the pressure from dropping unrealistically fast while we produce from the reservoir without injection. Specifically, the maximum pressure drop in the simulations for 10 years of production is kept below 2,500 psi. By comparison, assigning the same aquifer grid cells a porosity of one results in a pressure drop to atmospheric pressure in less than two years. Physically, this set-up corresponds to having either a thick or wide aquifer with enough volume to absorb some of the pressure response in relatively small subdomains.

As an example of coning in fractured heavy oil reservoirs, we use a fluid from a previous study in which the critical component properties are provided (Moortgat and Firoozabadi, 2013a). The initial composition and computed Fickian diffusion coefficients (used in the last example) are summarized in Table 1. We consider a reservoir temperature of 226°F and initial bottom hole pressure of 5,459 psi. For the coning study, phase behavior is not pronounced because the pressures remain well above the bubble-point pressure (740 psi) and there is no gas injection. Water will flow through the domain due to the coning process, but this involves immiscible two-phase flow. The main parameters that affect immiscible flow are the oil density, which is 0.976 g/cm³ and viscosity of 121 cp. This viscosity is taken from field data, but in one of the examples we also consider the degree of coning for lower oil viscosities of 80, 40, and 12 cp. Oil (and gas) viscosities are computed from the Lohrenz et al. (1964) approach and can be adjusted by tuning the critical volume of the residue (C_{12+}). We consider a water density of 0.971 g/cm³, and constant viscosity of 0.26 cp. The high oil-to-water viscosity ratio (a factor 471) is the critical parameter that causes the coning phenomenon.

In the matrix and the vugs we assume a quadratic relative permeability for oil and a cubic relation for water with a 50% residual oil saturation to water. The end-point relative permeabilities are 1 for oil and 0.3 for water. In the fractures we assume linear relative permeabilities with unit end-points as the base-case. We also investigate the sensitivity to different relations for both matrix and fracture relative permeabilities. In all but one of the examples we consider an oil-wet formation and neglect capillarity. In one example we show that capillary imbibition for a water-wet rock does not significantly change the results.

As a base-case, we produce at a constant rate of 5% pore volumes (PV) per year without injection. This rate is defined in terms of the total hydrocarbon (HC) PV in the fractures, vugs and matrix, and corresponds to about an order of magnitude range in volumetric production rates for the different domain sizes that we consider. We also consider the effect of lower production rates.

Before presenting our results, we point out a numerical subtlety: for a rectilinear network of fractures aligned with the coordinate axes, there is no gravitational (flux) component along the direction of perfectly horizontal fractures. This tends to underestimate the (buoyant component of) flow of fluids from horizontal into vertical fractures (and vice versa). To remedy this potential issue, we take advantage of the unstructured grid implementation of our higher-order finite element methods for flow and transport and consider domains with a small dip angle (with a fracture grid that is tilted by 2 degrees).

Results and Discussion

Water Coning in 2D 52 m × 200 m Fractured Cross-Section In the first set of simulations, we consider a 52 m × 200 m two-dimension subsection of the reservoir with 4 m × 4 m matrix blocks, surrounded by discrete fractures. The domain is discretized by 27 × 101 elements. This relatively small domain size allows us to do some preliminary parameter sensitivity studies, before considering larger domains. First, we consider the effect of the distance between the production well and the water-oil contact. We perform 4 simulations in which a single vertical well is placed on the right boundary (perforated by a fracture) at $z = 32, 80, 132,$ and 176 m above the water-oil contact. An additional simulation considers a perforated horizontal well over the full (top) width of the domain.

Figure 4 shows grid, the location of the production wells, and the water saturation throughout the domain at $t = 1$ yr for the 4 different depths of vertical wells, and for a horizontal well. We find that breakthrough of water occurs very early: after less than 2 weeks for the lowest well, and up to about one to two months for the vertical and horizontal wells in the top of the reservoir. After a year, water has reached nearly every fracture in the domain below the production well, albeit at low saturations ($< 1\%$).

Figure 5 shows the water saturation after producing for 5 years (at 5% HCPV/yr). For all cases breakthrough of water occurred early on, but for wells near the top of the reservoir, the water saturation near the wells is still manageable ($< 10\%$). We also observe a benefit from the rise of the water level in the bottom of the reservoir, which aids recovery of oil from the matrix blocks through gravity.

Water production and oil recovery for the above simulations are summarized in **Figure 6**. We see that some breakthrough of water occurs early in all cases, but that the increase in water saturation after initial breakthrough is quite different depending on the location of the production well. When the well is close to the water-oil contact, water production will increase significantly early on, but when the well is further from the water table (> 100 m), the produced water saturation increases only slowly. Interestingly, we find that there is early breakthrough, followed first by a period of near constant water production, and after about 6 years a second period of steeper increase in water production. This has also been observed in experiments where nC_5 was injected in a fractured stack saturated with nC_{14} (Firoozabadi and Markeset, 1994).

In terms of oil recovery, remember that the initial fraction of oil in the fractures is 20%, and 33% is in the fractures and the vugs. When the production well is close to the water-oil contact, significant water production occurs early on, and oil is mostly recovered from the relatively small area between the aquifer and the well. The oil recovery is less than the amount of oil in the fractures and vugs. On the other hand, if production is from the top, most of the oil in the fractures is eventually recovered.

The general (and obvious) conclusion is that placing the production wells as far away as possible from the aquifer reduces coning. We will therefore focus on either single (vertical) or horizontal wells in the top of the reservoir. From Figure 6 it may appear as if there is no significant difference in a single vertical well or a horizontal well in the top of the domain. However, this is mostly due to the relatively small width of the domain considered so far. For larger domains, we expect the water level to rise more slowly far away from the producer and the relative coning effect to be more significant. In that case, using horizontal wells maintains a maximum distance from the aquifer, while distributing the pressure drop over a wider area, thereby reducing the risk of significant coning with early breakthrough.

Effect of Matrix Block Size on Coning We investigate the effect of matrix block size (or, equivalently, fracture density) by performing two additional simulations for the same domain size, but with block sizes of 2×2 and 8×8 m², respectively. Assuming that oil is recovered mostly from the fractures, we maintained a similar amount of oil in the fractures by halving the fracture aperture in the former case and doubling the aperture in the latter. **Figure 7** compares the simulated water breakthrough and oil recovery to the 4×4 m² block base-case for 5 years of production. The results are quite similar. The variation is mostly due to different degrees of vuggyness, because we used the same cross-flow element widths (which represents the vugs) for all cases. As long as the *effective* permeability of the domain remains equal, a similar amount of oil resides in fractures and vugs, and the fracture network is relatively dense, we expect to see similar degrees of coning.

Two- Versus Three-Dimensional Simulations We explore the differences and similarities in 2D versus 3D simulations for the coning problem by considering a $52 \text{ m} \times 52 \text{ m} \times 200 \text{ m}$ domain with $4 \text{ m} \times 4 \text{ m} \times 4 \text{ m}$ matrix blocks and all other parameters as before. Production is at a constant rate of 5% HCPV/yr from a horizontal well along the top x -axis ($y = 0$ and $z = 200 \text{ m}$). The water saturation throughout the domain at $t = 1 \text{ yr}$ is shown in **Figure 8**, as well as for an equivalent 2D simulation. The results are similar, but the coning is slightly less severe in the 3D simulation in which matrix blocks are surrounded by 6 fractures rather than than 4 in 2D, resulting in a higher fraction of oil in the fractures and vugs. When the fraction of oil in fractures and vugs is kept the same (by reducing the fracture and CFE-element widths in 3D) by symmetry 2D simulations with a single producing grid cell are equivalent to 3D simulations with a single horizontal well (and a horizontal well in a 2D simulation would correspond to multilateral horizontal wells in 3D). This will be demonstrated further in the numerical examples for CO₂ injection. With this understanding, the remaining sensitivity studies will be carried out for 2D grids with a single producing grid cell.

Effect of Mobility Ratio on Coning While the oil viscosity of 121 cp is based on a specific fluid and reservoir conditions, we can explore the degree of coning under a broader range of conditions by adjusting the mobility ratio between water and oil. We consider two different scenarios. In the first, we reduce the oil viscosity to 80, 40 and 12 cp (i.e., by up to an order of magnitude) by tuning the critical volume of the residue (C_{12+}). In the second, we consider a different wettability in the fractures by reducing the end-point relative permeability of water in the fractures by an order of magnitude (to 0.1). The latter only reduces the mobility ratio in the fractures, while the former also improves gravitational drainage from the matrix blocks. **Figure 9** shows the water saturation at $t = 5 \text{ yrs}$ for these 4 cases, and the breakthrough curves and oil recoveries are presented in **Figure 10**. We find that a lower water relative permeability in the fractures and a lower oil viscosity of 80 cp only marginally improve the results. However, for oil viscosities of 40 and 12 cp, water breakthrough is delayed by ~ 2 and 5 years, respectively. Oil recovery is more than doubled between the 121 and 12 cp cases. This is not only due to reduced coning, but also because of more efficient drainage from the matrix blocks with a final oil recovery higher than the initial oil in the fractures and vugs.

Effect of Matrix Wettability and Permeability Next, we consider the effect of rock properties on the degree of coning. We perform a simulation with the same capillary pressure curve as in Figure 1 for a water-wet rock and 3 additional simulations (without capillarity) for matrix permeabilities of 10, 100, and 1000 md. The water saturations at $t = 5 \text{ yr}$ are given in **Figure 11** and the water breakthrough and oil recovery in **Figure 12**. We find that due to the low oil mobility, capillary imbibition does not significantly affect the results. We

also considered a range of different water and oil relative permeabilities in the matrix, but found that this has a negligible impact on the results, due to the low matrix permeability and high oil viscosity.

Increasing the matrix permeability by one or two orders of magnitude is also insufficient to overcome the adverse mobility ratio of a factor ~ 500 . Only for a matrix permeability of 1000 md do we see a significant reduction in water production, and associated increase in oil recovery. The final oil recovery for that case is similar to that for a ten times lower mobility ratio ($\mu_o = 12$ cp) in Figure 10.

Effect of Domain Size and Production Rate In the final study of coning, we consider both a domain that is 4 times wider (400×200 m²), and one that has a two times thicker oil column (52×400 m²). The matrix blocks in all cases are 4 m \times 4 m. We also model the effect of production rates with 0.625%, 1.25%, 2.5%, and 5% PV/yr for the wider domain and 2.5%, and 5% PV/yr for the taller domain. We find that for all domain sizes and production rates water has invaded most of the fractures after a year (**Figure 13**), although to a lesser extent for lower production rates. **Figure 14** for the water production curves and oil recoveries shows that water production is of course reduced for the thicker oil column (with the production well further above the water aquifer) and for lower production rates, while for the wider domain the coning is more severe. The degree of coning is reduced for lower production rates, which result in lower pressure gradients (the pressure declines over time are also shown in Figure 14). We see that when the rate is halved the oil recovery is reduced only slightly due to the lower water production. The implication is that in field applications the production rate can be reduced to alleviate surface facilities for water separation due to coning, while maintaining reasonable oil production performance.

Effect of Local Viscosity Reduction around Production Wells One option that has been considered to reduce the coning problem, is to spray surfactants or ionic liquids around producing well-bores to reduce the local oil viscosity and associated pressure drop (Subramanian et al., 2015). We have carried out simulations to study whether this approach would indeed mitigate the coning problem. To model a 'best case scenario', we artificially reduced the oil viscosity considerably to 3.6 cp in a 10 m radius around the producing grid-cells and observed what affect this has on the degree of coning. However, we found that this treatment does not significantly reduce coning or improve oil recovery (results are similar enough that they are not shown in figures). The reason why such a local viscosity reduction does not have a significant impact on coning and oil recovery relates to the pressure profile throughout the domain. Reducing the viscosity in the near-well region only reduces the pressure drop somewhat in that region. The pressure profile *throughout* the domain is determined by the production rate; the reduction in viscosity and pressure drop near the producer is not 'felt' far away at the water-oil contact. Our general conclusion is that reducing the pressure in the near-well region may improve practical productivity constraints, but does not prevent the coning of water. Instead of reducing the oil viscosity, it is also possible to *increase* the water viscosity through polymers or gel, but this is unpractical for a large underlying aquifer.

CO₂ Injection and Fickian Diffusion Oil recovery from certain densely fractured heavy oil reservoirs may be enhanced considerably through CO₂ injection. When roughly equal volumes are injected and produced, the pressure gradients throughout the reservoirs are much smaller than for production without injection and water coning is **generally less severe, as long as the production wells are sufficiently far above an underlying aquifer**. The density difference between CO₂ (0.65 cm³/g) and the heavy oil is much larger than for water, which aids gravitational drainage. More importantly, CO₂ has a high solubility in this oil (75 mol%) and when it mixes with the oil, it leads to considerable swelling of the oil volume (up to 40%), and, most interestingly, a viscosity reduction to as low as 4 cp. The

combination of these favorable phase behavior effects can significantly improve oil recovery, which we demonstrated in an earlier work through 2D simulations (Moortgat and Firoozabadi, 2013a). Here we extend this problem to a 3D discretely fractured domain to contrast the high efficiency of CO₂ injection to the adverse coning issues related to depletion, as discussed above. We compare 3D simulations to 2D results, perform simulations with and without modeling Fickian diffusion, and compare results to a commercial dual-porosity simulator.

We first consider an optimal scenario in which the matrix blocks are small and the fractures densely spaced, before modeling CO₂ injection in the same domain as for the coning study. Specifically, we study a densely fractured domain with $40 \times 40 \times 40$ cm³ matrix blocks, surrounded by cross-flow elements that represent fractures and connected vugs. To facilitate fine mesh simulations, we consider a $10 \times 1.2 \times 10$ m³ 3D subsection, such that we have 3 matrix blocks in the y -direction and 25 blocks in the x - and z -directions. We perform simulations on two different grids: Grid 1 ($51 \times 11 \times 51$) and Grid 2 ($99 \times 13 \times 99$) elements, which have $\sim 90,000$ and $\sim 400,000$ degrees of freedom (faces) in our pressure solution. **Figure 15** shows Grid 2, as well as a 99×99 element 2D cross-section. A subtlety in comparing 3D to 2D simulations, as mentioned for the 3D coning simulations, is that for a given fracture/CFE width the fractional pore volume in the fractures and vugs will be larger in the 3D set-up (with fractures surrounding 6 sides of each matrix cube) than in the 2D case (fractures on 4 sides of each rectangular matrix block). In most applications the amount of oil in the fractures is small compared to that in the matrix and this is not an issue. However, in this particular triple-porosity reservoir the majority of oil may reside in the fractures and vugs, so we have to be careful in constructing our numerical representation. Specifically, for the 3D case we consider 1 mm fracture apertures and 10 cm wide CF elements (accounting for connected vugs), while in the 2D simulations we have 1.5 mm fracture apertures and 17 cm wide CF elements. With this set-up, 9% of the oil resides in the fractures alone while 67.5% is contained in the fractures and vugs together (the high end of estimates for this reservoir).

The domain is initially saturated with the same heavy oil as in the coning study and at the same initial temperature and pressure. The CO₂ density at reservoir conditions is given above and the viscosity is 0.035 cp. We consider a residual oil saturation of 50% and quadratic relative permeabilities with end-point relative permeabilities of 0.4 for both oil and gas. The gas end-point relative permeability is low because CO₂ is believed to alter the wettability (Moortgat et al., 2013; Müller, 2011). This change in wettability can be partly accounted for by end-point relative permeabilities. Because of the high solubility of CO₂ in this oil, and the high reservoir pressure, capillary pressure is negligible in this problem, while Fickian diffusion is critical. The full matrix of (composition dependent) diffusion coefficients for the initial oil are provided in Table 1.

In our simulations, CO₂ is injected at a constant rate of 25% PV/yr from the top right (from a horizontal well for the 3D case) with constant pressure production from the bottom left. **Figure 16** shows the molar fraction of CO₂ throughout the domain at 100% PVI for simulations without and with consideration of Fickian diffusion and for both 2D and 3D simulations. For the latter, we compared a cross-section of a fine 3D grid to 2D results. We find that without diffusion, recovery is mainly from the fractures and vugs with much slower recovery from the matrix blocks through gravitational drainage. For CO₂ injection, a dense network of fractures is beneficial, because it offers a large interaction surface between the fractures and the matrix through which species can transfer driven by Fickian diffusion. The CO₂ that diffuses into the matrix blocks lead to swelling of the oil, which expels it from the tight matrix, and significantly reduces the oil viscosity, aiding gravitational drainage. The extent of the latter effect is clear from **Figure 17** which shows the viscosity

throughout the domain for simulations with and without diffusion. Without diffusion, the viscosity reduction mostly affects the oil in the fractures and vugs, while through diffusion the viscosity is reduced to less than 10 cp in most of the domain.

The benefits from CO₂ injection and the importance of Fickian diffusion are clear from the recovery plots in **Figure 18a**, which shows results on 2D and both 3D grids and with and without Fickian diffusion. Recovery is high both with and without diffusion, because a large fraction of the oil resides in the fractures and vugs from which it is readily recovered. Diffusion, however, facilitates significant recovery of matrix oil beyond gravitational drainage, which provides 20% incremental recovery. When the fraction of oil in the matrix blocks is higher, Fickian diffusion can more than double the oil recovery as demonstrated below. Figure 18 also shows that the 3D results on both Grid 1 and 2 have converged, and that simulations on a 2D cross-section can accurately predict those from a full 3D simulation. The latter is somewhat unexpected, because in 3D the surface area between the fractures and matrix is larger than in the 2D representation. The good agreement is most likely due to the small matrix blocks considered here, which are quickly saturated with CO₂. For much larger matrix blocks the diffusive propagation front of CO₂ into the matrix may be more sensitive to the surface area.

To correctly predict oil recovery from CO₂ injection in densely fractured reservoirs, one needs a self-consistent model for Fickian diffusion that can account for the diffusive flux between gas in the fractures and single-phase oil in the matrix blocks. Most reservoir simulators rely on a diagonal matrix of constant self-diffusion coefficients and ad hoc approximations to calculate the diffusive flux between neighboring grid cells that are each in a different single-phase. However, recently, Halliburton has implemented our improved diffusion model into their next-generation Nexus simulator. We used the implicit dual-porosity-single-permeability option in Nexus to simulate the example in Moortgat and Firoozabadi (2013a) with 1 mm wide fractures and 2 cm wide CFE elements in our discrete fracture model, such that only 8% of the oil resides in fractures and vugs. The dual-porosity results depend on which shape-factor is chosen. We considered three different shape factors, referred to as σ_1 (Kazemi et al., 1976), σ_2 (Lim and Aziz, 1995), and σ_3 (Coats, 1989), which are given in terms of the effective size of the matrix blocks as:

$$\sigma_1 = \frac{4}{L^2}, \quad \sigma_2 = \frac{\pi^2}{L^2}, \quad \sigma_3 = \frac{8}{L^2} \quad \text{with,}$$

$$\frac{1}{L^2} = \left(\frac{1}{L_x^2} + \frac{1}{L_y^2} + \frac{1}{L_z^2} \right) = 18.75 \text{ m}^{-2} \quad (1)$$

Figure 18b compares the oil recoveries with and without diffusion for both simulators. The purely convective dual-porosity results are insensitive to the choice of shape factor, while we find that both the Lim and Aziz (1995) and Coats (1989) shape factors provide reasonably similar oil recoveries to our discrete fracture results with diffusion. The differences may be partly due to our sub-matrix block grid resolution, which allows the CO₂ front to penetrate the matrix blocks earlier and more effectively, even without diffusion (as can be seen in Figures 5 and 6 in Moortgat and Firoozabadi (2013a)). While we cannot determine the exact source of the discrepancy between our model and Nexus, the difference is already present in the comparison of the purely convection cases. The key point is that the incremental recovery due to diffusion for the two models is roughly the same.

Two other widely used commercial reservoir simulators were unable to reproduce these results due to the representation of diffusion, fractures and/or phase behavior.

CO₂ Injection into Fractured Domain with Underlying Aquifer As a last example, we model CO₂ injection in the same base-case 52 × 200 m² domain as in the coning study and with the same 4 × 4 m² matrix blocks (e.g., 100× larger). The fracture apertures and all other rock and fluid properties are the same as in that example. CO₂ is injected at 2.5% PV/yr from the top-right corner and production is from the left, 100 m above the water-oil contact, as indicated in **Figure 19**, which shows the CO₂ molar fraction and oil viscosity throughout the domain at 30% PVI for simulations without and with Fickian diffusion. **Figure 20** shows the corresponding oil recovery and molar fraction of CO₂ in the production stream, as well as results for an injection rate of 5% PV/yr. The results are remarkably similar to those for the smaller domain with smaller matrix blocks. Due to diffusion, CO₂ is able to fully saturate the matrix blocks, improve the matrix oil properties through phase behavior, and increase oil recovery by a factor of three. Without diffusion, the oil recovery as a function of pore volume injected does not show a dependence on the injection rate, while the effectiveness of diffusion is greater for lower injection rates, which give diffusion more time to compete with advective flow through the fracture network. These results suggest that even at the field scale, CO₂ injection in fractured reservoirs may be highly beneficial.

We note that the qualitative results from our CO₂ injection study apply to a broader pressure range: for pressures from 3,000 to 6,000 psi, the CO₂ solubility in this oil varies from 65 to 74 mol%, the initial oil viscosity ranges from 90 to 130 cp and the fully CO₂-saturated oil ranges from 6.4 cp down to 4.7 cp, respectively. In other words, for a wide range of pressures, the CO₂ solubility is high and the viscosity reduction significant. For much lower *temperatures*, e.g. at 70° F, the CO₂ solubility is still 54 mol%, but both the initial oil viscosity and the fully saturated oil viscosity increase significantly and even oil production through CO₂ injection may prove ineffective.

Conclusions

In this work we studied challenges related to the production of heavy viscous oil from fractured and vuggy reservoirs with a strong underlying aquifer. In reservoirs with a tight (low permeability) matrix rock saturated with viscous oil, gravitational drainage and capillary imbibition of matrix oil during depletion or waterflooding is slow and oil is mostly recovered from fractures and connected vugs. For such reservoirs to be attractive for hydrocarbon production, a large fraction of the oil should reside in these high permeability conduits for flow. We consider reservoirs in which 20-50% of the oil is contained in fractures and vugs, which also make up the bulk of the effective permeability of ~ 1 d (for a fracture permeability of 100 d). As a base-case, we consider a matrix permeability and (intrinsic) porosity of 1 md and 8%, respectively, an oil viscosity of 121 cp. Because water has a much lower viscosity than the oil, there is an inherent risk of coning when oil is produced from reservoirs with an underlying aquifer.

The numerical investigations in this work were performed with our higher-order finite element reservoir simulator, which incorporates a discrete fracture model based on the cross-flow equilibrium approach. The performance of our simulator was first demonstrated by modeling a set of experiments in which water was injected at different rates into a stack of chalk blocks separated by a number of discrete fractures. We found excellent agreement between the experimental and simulated results, which show that at low injection rates capillary imbibition of water from the fractures into the matrix blocks can be so efficient that the water fronts in the fractures and the matrix propagate at the same rate, resulting in near piston-like displacement of matrix oil. In earlier work (Moortgat and Firoozabadi, 2013c,b), we showed that the same is true at the reservoir scale as long as the matrix blocks are sufficiently small. This numerical

experiment highlights the high CPU efficiency of our model compared to a control volume finite difference method that was used to model this same experiment (Monteagudo and Firoozabadi, 2007).

We then studied the risk and degree of coning when oil is produced without injection from a densely fractured heavy oil reservoir with an underlying aquifer, as well as the potential of CO₂ injection as an enhanced oil recovery strategy.

For the coning study, we carried out an extensive parameter study, investigating the impacts of 1) production well types and placement, 2) domain sizes, 3) oil viscosity, 3) water and oil relative permeabilities in the matrix, 4) relative permeability in the fractures, 5), capillary pressures (wettability), 6) matrix permeability, 7) matrix block sizes, 8) production rates (or, equivalently, pressure gradients), and 9) a local viscosity reduction around producing well-bores. Our conclusions related to coning can be summarized as follows:

1. For all parameters considered, breakthrough of water occurs early on but the amount of water production at later times depends on rock and fluid properties. The amount of water production may remain manageable for years before increasing again.
2. Coning was not significantly affected by varying the matrix block sizes from 2 m × 2 m to 4 m × 4 m and 8 m × 8 m.
3. For low matrix permeabilities, coning and oil recovery are insensitive to water and oil *relative* permeabilities in the matrix.
4. A reduction of water mobility (only) in the fractures by an order of magnitude only modestly delayed the early breakthrough of water and improved oil recovery by ~ 12% incremental.
5. The degree of coning (and resulting poor oil recovery) for a 80 cp oil was found to be similar to the 121 cp base-case. For 40 cp and 12 cp oils, breakthrough is delayed by 2 and 5 years, respectively, and oil recovery is 1.5 to 2 times higher.
6. Capillary pressures did not significantly affect the process under the conditions of this study.
7. Increasing the matrix permeability from 1 md to 10 and 100 md only marginally improved the results. For a matrix permeability of 1000 md, water breakthrough still occurred very early on, but water saturations in the production streamer stayed below 2% for about 5 years and below 5% for most of the 10 years of production. Oil recovery was about twice that of the base-case.
8. For a thicker oil column with production wells in the top, coning is obviously reduced.
9. Reducing the oil viscosity around wells (by spraying surfactants or ionic liquids) may improve productivity, but does not significantly reduce coning because it does not affect the pressure gradients at the water-oil contact.
10. High production rates increase the degree of coning. Similar oil recovery can be achieved at reduced production rates, due to the lower amount of water production.
11. Well placement and types: coning can be reduced by increasing the production well surface area, placed far above the water-oil contact. Horizontal wells are preferable to vertical ones, and multilateral horizontal wells are an improvement over single wells.

For our investigation of CO₂ injection in densely fractured rock we first presented simulation results for relatively small and densely fractured 2D and 3D domains with small matrix blocks of 0.4 m × 0.4 m (× 0.4 m) with the same rock and fluid parameters as the coning study. This showed that we can obtain the same predictions from 2D simulations as from 3D simulations and demonstrated the

convergence of our higher-order schemes on coarse grids. We also compared our results to those of a commercial reservoir simulator that uses our same model for Fickian diffusion. Finally, we verified that the promising results from our small-scale domains carry over to the same domain size as the coning examples with an underlying aquifer and 100 times larger matrix blocks.

The advantages of CO₂ injection over depletion or water flooding from densely fractured reservoirs are:

1. Fickian diffusion can drive species exchange between CO₂-rich gas in the fractures and oil in the matrix blocks, and diffusion does not depend (directly) on the low matrix permeability.
2. The degree of Fickian diffusion depends on the size of the gas-oil interface. A densely fractured formation is actually beneficial for mass transfer between and oil phases.
3. CO₂ is particularly promising because it often has a high solubility in oil and can lead to favorable phase behavior. For the oil considered in this study, the CO₂ solubility is 75 mol%, and dissolution leads to up to 40% volume swelling and an oil viscosity reduction by a factor 25. This favorable phase behavior is not shared by other injection gasses, such as nitrogen, which has been injected in off-shore fractured reservoirs.
4. CO₂ also has a low density at the high reservoir pressure, which improves gravitational drainage of oil from the matrix blocks, as compared to waterflooding.
5. Due to the combined processes of Fickian diffusion and phase behavior, we find that a significant amount of matrix oil can be recovered, while simulations without diffusion show mostly production of the oil in the fractures and vugs.

Whether CO₂ injection is a feasible option for enhanced oil recovery depends on availability and cost of a CO₂ supply.

Acknowledgements

We appreciate the help of Saeedeh Mohebbinia and Terry Wong at Halliburton in carrying out the simulations with the Nexus reservoir simulator, and Halliburton's permission to publish these results.

References

- Abass, H., Bass, D., 1988. The Critical Production Rate in Water-Coning System, Paper SPE-17311-MS presented at the Permian Basin Oil and Gas Recovery Conference, 10-11 March, Midland, Texas. doi: 10.2118/17311-MS.
- Beveridge, S., Coats, K., Alexandre, M., 1970. Numerical Coning Applications. *J. Can. Pet. Tech.* **9** (3):209–215.
- Chaney, P., Noble, M., Henson, W., Rice, T., 1956. How to Perforate Your Well to Prevent Water and Gas Coning. *Oil Gas J.* **55**:108.
- Coats, K., 1989. Implicit Compositional Simulation of Single-Porosity and Dual-Porosity Reservoirs, Paper SPE 18427 presented at 10th SPE Symp. Reservoir Simulation, Houston, Texas, Feb. 6-8.
- Firoozabadi, A., Markeset, T., 1994. Miscible Displacement in Fractured Porous Media: Part I — Experiments, Paper SPE/DOE 27743 presented at the SPE/DOE Ninth Symposium of Improved Oil Recovery held in Tulsa Oklahoma, 17-20 April.

- Firoozabadi, A., Thomas, L., 1990. Sixth SPE Comparative Solution Project: Dual-Porosity Simulators. *SPE J.* **42** (6):710–763.
- Geiger, S., Matthäi, S., Niessner, J., Helmig, R., 2009. Black-Oil Simulations for Three-Components, Three-Phase Flow in Fractured Porous Media. *SPE J.* **14** (2):338–354. doi: 10.2118/107485-PA.
- Giger, F.M., 1989. Analytic Two-Dimensional Models of Water Cresting Before Breakthrough for Horizontal Wells. *SPE J.* **4** (4): 409–416.
- Hoteit, H., Firoozabadi, A., 2005. Multicomponent Fluid Flow by Discontinuous Galerkin and Mixed Methods in Unfractured and Fractured Media. *Water Resour. Res.* **41** (11). doi: 10.1029/2005WR004339.
- Hoteit, H., Firoozabadi, A., 2006. Compositional Modeling of Discrete-Fractured Media without Transfer Functions by the Discontinuous Galerkin and Mixed Methods. *SPE J.* **11** (3):341–352. doi: 10.2118/90277-PA.
- Hoteit, H., Firoozabadi, A., 2008. An Efficient Numerical Model for Incompressible Two-Phase Flow in Fractured Media. *Adv. Water Resour.* **31** (6):891–905. doi: 10.1016/j.advwatres.2008.02.004.
- Jiang, Q., Butler, R., 1998. Experimental And Numerical Modelling of Bottom Water Coning to a Horizontal Well. *J. Can. Pet. Tech.* **37** (10):82–91.
- Kazemi, H., Merrill, L., Porterheld, K., Zeman, P., 1976. Numerical simulation of water-oil flow in naturally fractured reservoirs. *SPE J.* **16** (6):317–326.
- Letskeman, J., Ridings, R., 1970. A Numerical Coning Model. *SPE J.* **10** (4):418–424.
- Lim, K., Aziz, K., 1995. Matrix-Fracture Transfer Shape Factors for Dual-Porosity Simulators. *J. Pet. Sci. Eng.* **13**:169–178.
- Lohrenz, J., Bray, B.G., Clark, C.R., 1964. Calculating viscosities of reservoir fluids from their compositions. *J. of Pet Technol* **16** (10): 1171–1176.
- Monteagudo, J.E.P., Firoozabadi, A., 2007. Control-Volume Model for Simulation of Water Injection in Fractured Media: Incorporating Matrix Heterogeneity and Reservoir Wettability Effects. *SPE J.* **12** (3):355–366. doi: 10.2118/98108-PA.
- Moortgat, J., Firoozabadi, A., 2010. Higher-Order Compositional Modeling with Fickian Diffusion in Unstructured and Anisotropic Media. *Adv. in Water Resour.* **33** (9):951 – 968. doi: 10.1016/j.advwatres.2010.04.012.
- Moortgat, J., Firoozabadi, A., 2013a. Fickian Diffusion in Discrete-Fractured Media from Chemical Potential Gradients and Comparison to Experiment. *Energ. Fuel* **27** (10):5793–5805. doi: 10.1021/ef401141q.
- Moortgat, J., Firoozabadi, A., 2013b. Higher-Order Compositional Modeling of Three-Phase Flow in 3D Fractured Porous Media Based on Cross-Flow Equilibrium. *J. Comput. Phys.* **250** (0):425 – 445. doi: <http://dx.doi.org/10.1016/j.jcp.2013.05.009>.
- Moortgat, J., Firoozabadi, A., 2013c. Three-Phase Compositional Modeling With Capillarity in Heterogeneous and Fractured Media. *SPE J.* **18** (6):1150–1168.

- Moortgat, J., Firoozabadi, A., Li, Z., Espósito, R., 2013. CO₂ Injection in Vertical and Horizontal Cores: Measurements and Numerical Simulation. *SPE J.* **18** (2):331–344.
- Moortgat, J., Li, Z., Firoozabadi, A., 2012. Three-Phase Compositional Modeling of CO₂ Injection by Higher-Order Finite Element Methods with CPA Equation of State for Aqueous Phase. *Water Resour. Res.* **48**:W12511.
- Müller, N., 2011. Supercritical CO₂-Brine Relative Permeability Experiments in Reservoir Rocks — Literature Review and Recommendations. *Transport Porous Media* **87** (2):367–383. doi: 10.1007/s11242-010-9689-2.
- Muskat, M., Wyckoff, R., 1935. An Approximate Theory of Water Coning in Oil Production. *Trans., AIME* **114**:144–161.
- Pérez-Martínez, E., Rodríguez de la Garza, F., Samaniego-Verduzco, F., 2012. Water Coning in Naturally Fractured Carbonate Heavy Oil Reservoir - A Simulation Study, Paper 152545-MS presented at the SPE Latin America and Caribbean Petroleum Engineering Conference, 16-18 April, Mexico City, Mexico.
- Pooladi-Darvish, M., Firoozabadi, A., 2000. Experiments and Modeling of Water Injection in Water-Wet Fractured Porous Media. *J. Can. Pet. Tech.* **39** (3):31–42.
- Saffman, P., G.I., T., 1958. The Penetration of a Fluid into a Porous Medium or Hele-Shaw Cell Containing a More Viscous Liquid. *Pro. Roy. Soc. A* **245**:312–329.
- Schols, R., 1972. An Empirical Formula for the Critical Oil Production Rate. *Erdoel Erdgas, Z.* **88** (1).
- Settari, A., Aziz, K., 1974. A Computer Model for Two-Phase Coning Simulation. *SPE J.* **14** (3):221–236.
- Singhal, A., 1996. Water And Gas Coning/Cresting A Technology Overview. *J. Can. Pet. Tech.* **35** (4):56–62.
- Subramanian, D., Wu, K., Firoozabadi, A., 2015. Ionic Liquids as Viscosity Modifiers for Heavy and Extra-Heavy Crude Oils. *Fuel* **143**:519–526.
- Tan, C., Homsy, G., 1986. Stability of Miscible Displacements in Porous Media: Rectilinear Flow. *Phys Fluids* **29** (11):3549–3556.
- Verga, F., Viberti, D., Di Renzo, D., 2005. Are Multilateral Wells Really Effective To Control Water Coning?, Paper OMC-2005-055 Presented at the SPE Offshore Mediterranean Conference and Exhibition, 16-18 March, Ravenna, Italy.
- Warren, J., Root, P., 1963. The Behavior of Naturally Fractured Reservoirs. *SPE J.* 245–44.

Table 1: Initial oil compositions (z_i in mol%) for $n_c = 8$ (pseudo-)components and effective diffusion coefficients ($\phi D_{ij} \times 10^{-12}$ m²/s (with $i, j = 1, \dots, n_c - 1$ and ϕ the porosity).

z_i		CO ₂	N ₂	H ₂ S	C ₁	C ₂₋₃	C ₄₋₆	C ₇₋₁₁
5.96	CO ₂	82.24	-1.77	-2.05	-3.08	-1.42	-0.51	0.30
1.80	N ₂	-0.29	93.43	-0.49	-0.88	-0.32	-0.0008	0.31
8.09	H ₂ S	-1.27	-1.79	98.31	-3.68	-1.52	-0.43	0.47
7.13	C ₁	-1.21	-2.04	-2.069	114.84	-1.50	-0.43	0.55
7.91	C ₂₋₃	-1.32	-1.972	-2.44	-3.90	88.00	-0.67	0.26
11.12	C ₄₋₆	-2.74	-3.50	-4.47	-6.40	-3.50	69.21	-0.78
11.46	C ₇₋₁₁	-4.06	-4.72	-5.99	-7.84	-4.93	-3.36	51.25
46.52	C ₁₂₊							

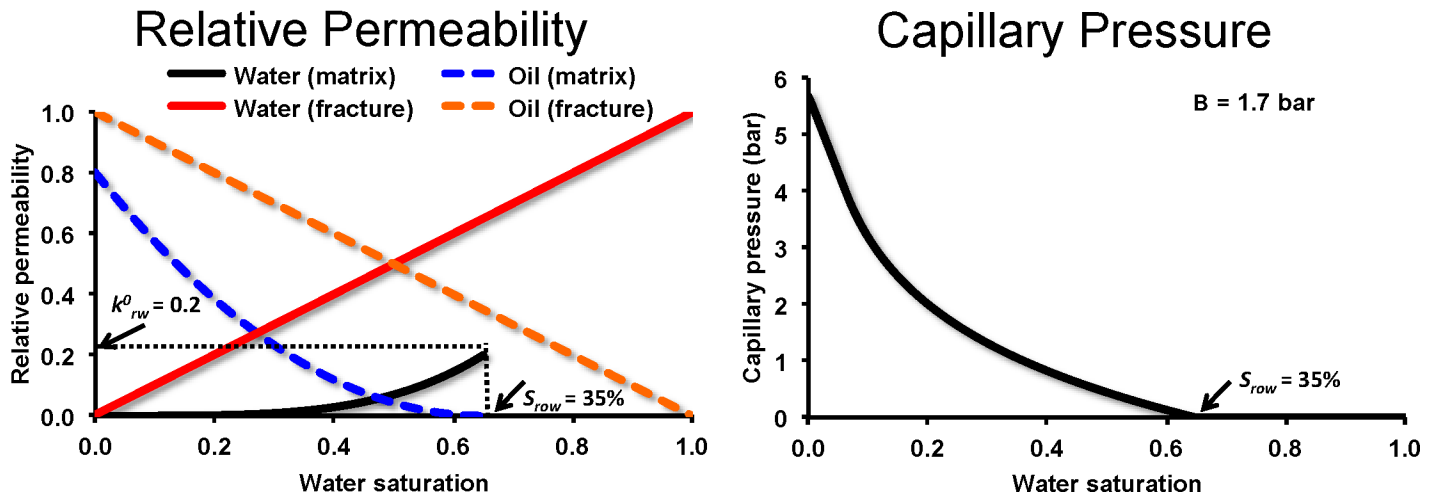


Figure 1: Relative permeabilities are linear with unit end-points in the fracture. In the matrix, the water relative permeability has an exponent of 4 and end-point of 0.2, while the oil relative permeability is quadratic with end-point 0.8. The residual oil saturation is $S_{row} = 35\%$. The water-oil capillary pressure in the matrix is $p_c(\text{bar}) = -B \ln S_{w,\text{eff}}$ with $B = 1.7$ bar, and is linearly extrapolated for effective water saturations ($S_{w,\text{eff}} = S_w / (1 - S_{or})$) below 0.1 for numerical stability. Because the capillary pressure scales with $\sqrt{\phi/K}$, the capillary pressure in the fractures is effectively zero (because the fracture permeability is 6×10^5 times the matrix permeability).

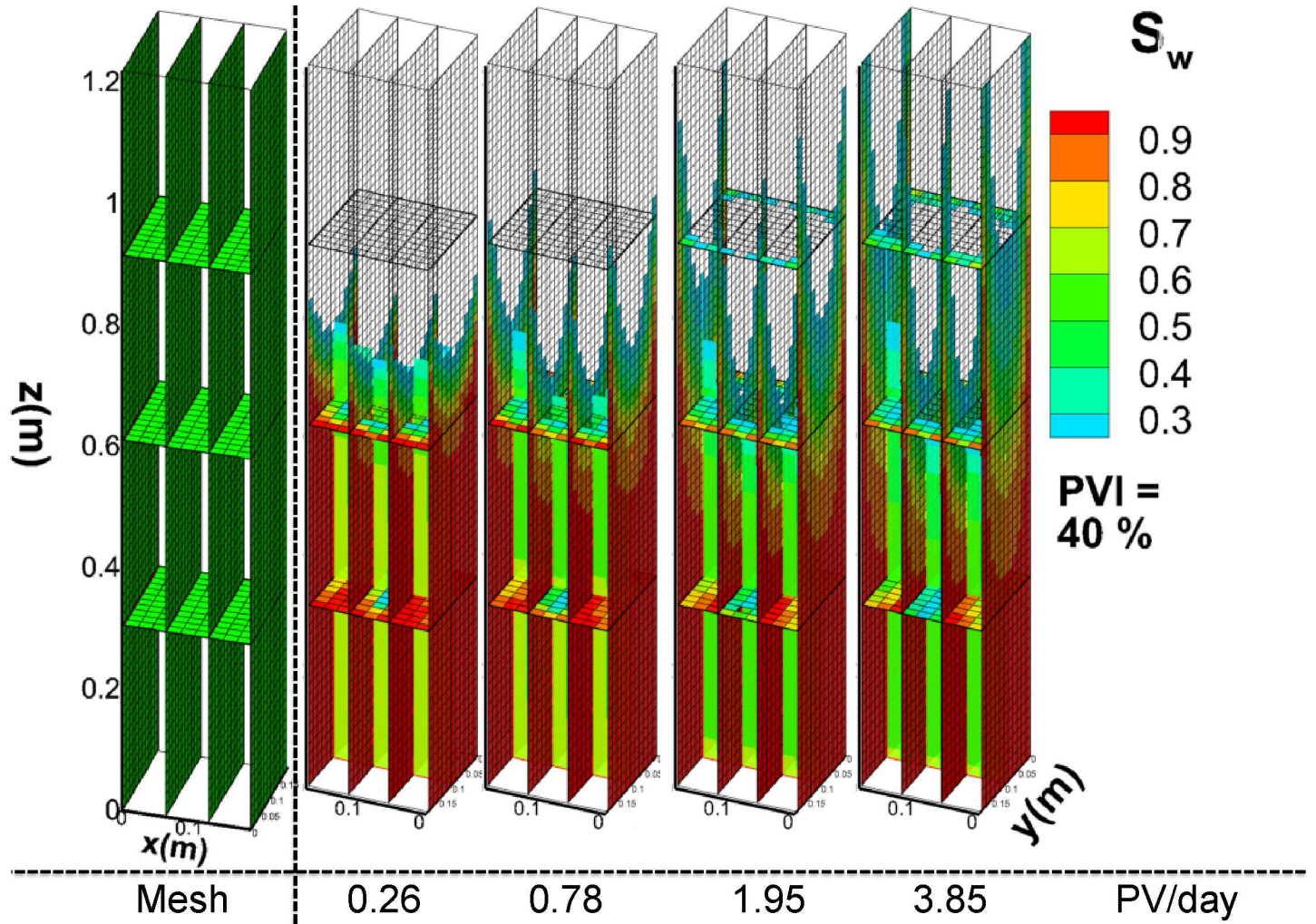


Figure 2: Configuration of the fractured stack in the Pooladi-Darvish and Firoozabadi (Pooladi-Darvish and Firoozabadi, 2000) experiments, and Grid 2 ($13 \times 13 \times 79$ elements) used for the modeling (left). The fractures at the top, bottom, front and back are omitted for a more clear visualization. Water saturation (right 4 panels) at 40% PV of water injection at 0.26, 0.78, 1.95, and 3.85 PV/day, projected on slices through 4 vertical and 3 horizontal fractures.

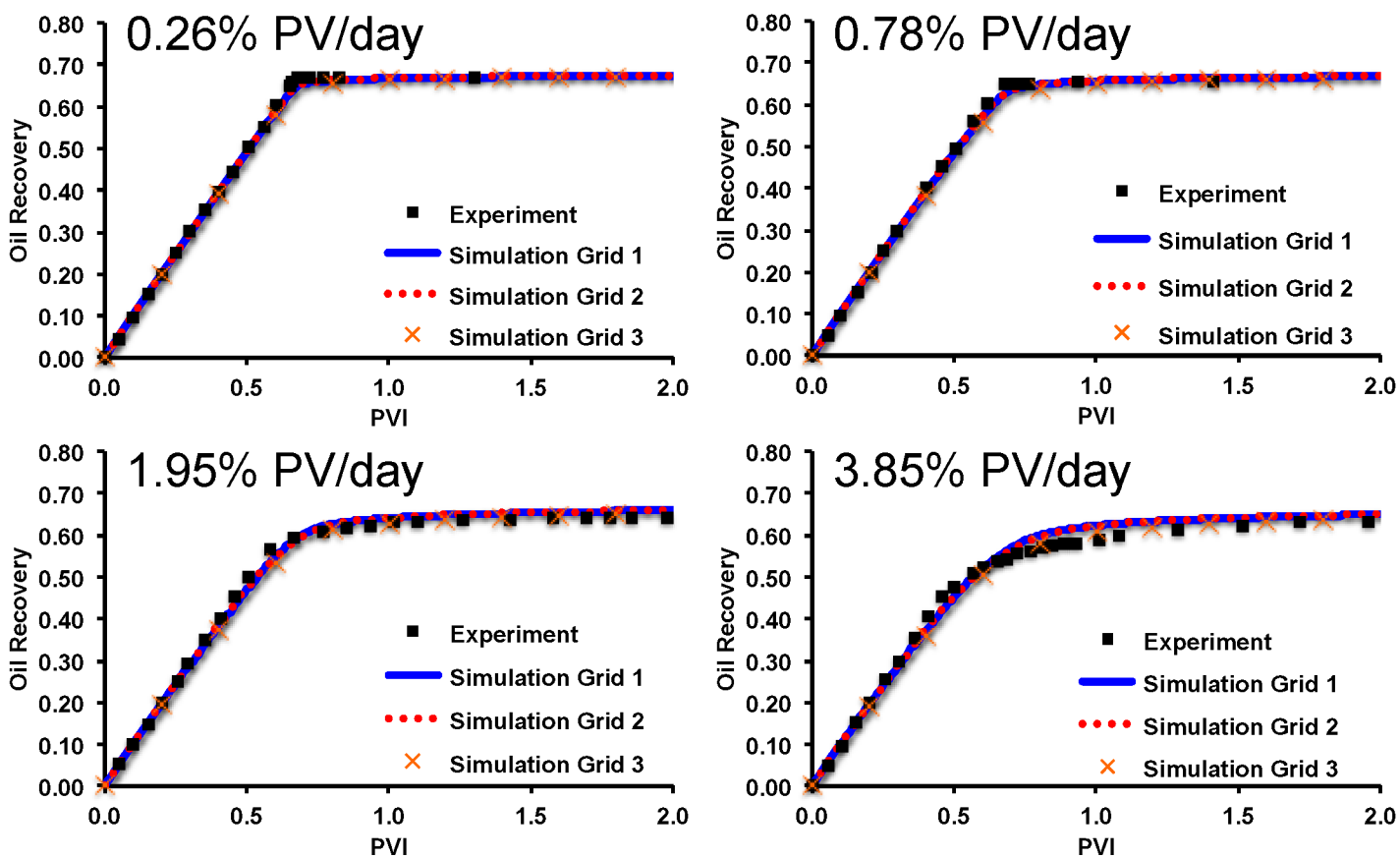


Figure 3: Oil recovery for water injection at 0.26, 0.78, 1.95, and 3.85 PV/day. Experimental data points and simulations results on Grid 1 (13 × 7 × 41), Grid 2 (13 × 13 × 79), and Grid 3 (7 × 6 × 29).

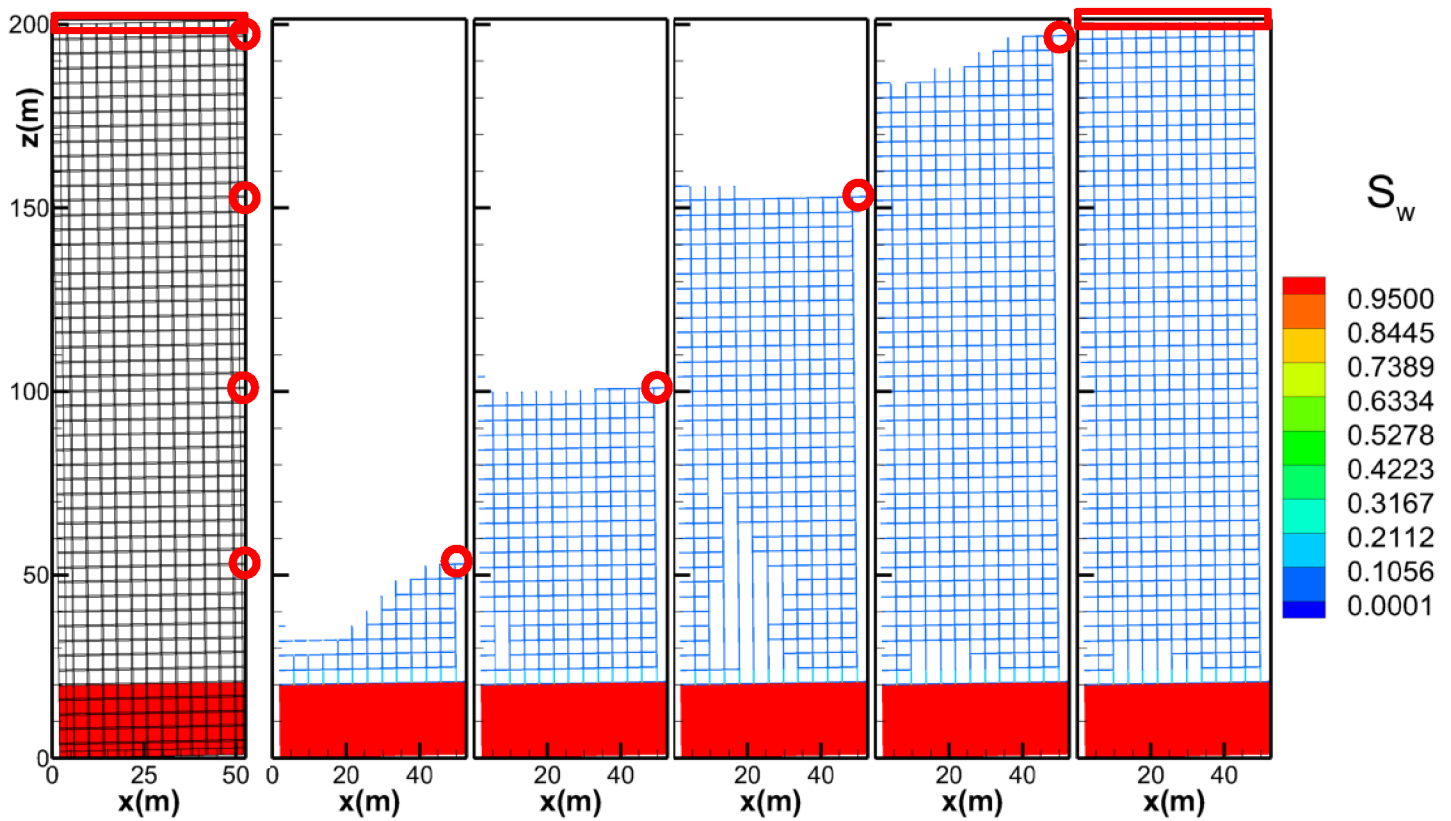


Figure 4: 27×101 element grid for $52 \text{ m} \times 200 \text{ m}$ domain with $4 \text{ m} \times 4 \text{ m}$ matrix blocks and 40 cm CFE elements (left). Red circles indicate the location of vertical production wells for 4 different simulations, the red rectangle indicates the location of a horizontal well, and the red grid cells represent the aquifer. Water saturation are shown (right 5 panels) for simulations in which a vertical production well penetrates to a distance z from the water-oil contact, for $z = 32, 80, 132,$ and 176 m as indicated by circles. The right-most is for a horizontal well spanning the width of the domain. Results are shown at $t = 6$ months.

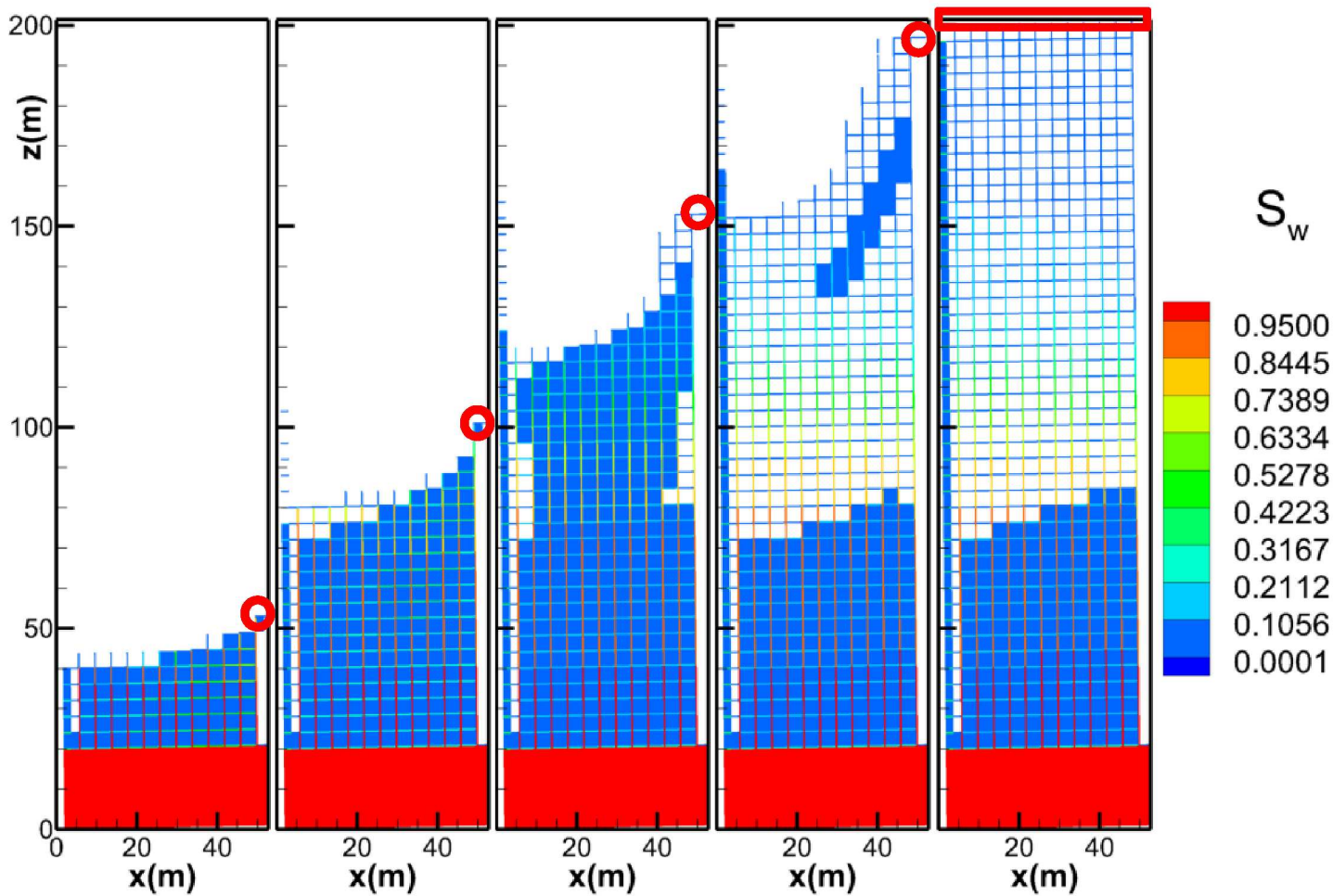


Figure 5: Same as Figure 4 but at $t = 5$ years.

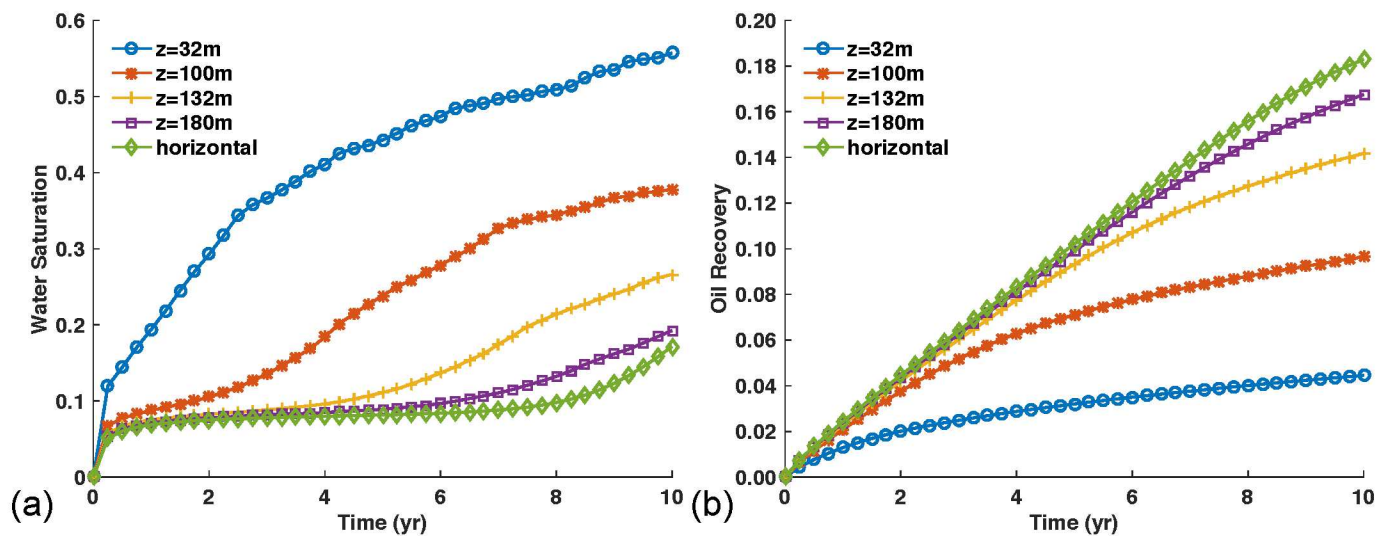


Figure 6: Water saturation in the production well (a) and oil recovery (b) for simulations in which a vertical production well penetrates to a distance z from the water-oil contact, for $z = 32, 80, 132,$ and 176 m, and for a horizontal well in the top. Domain size is 52×200 m².

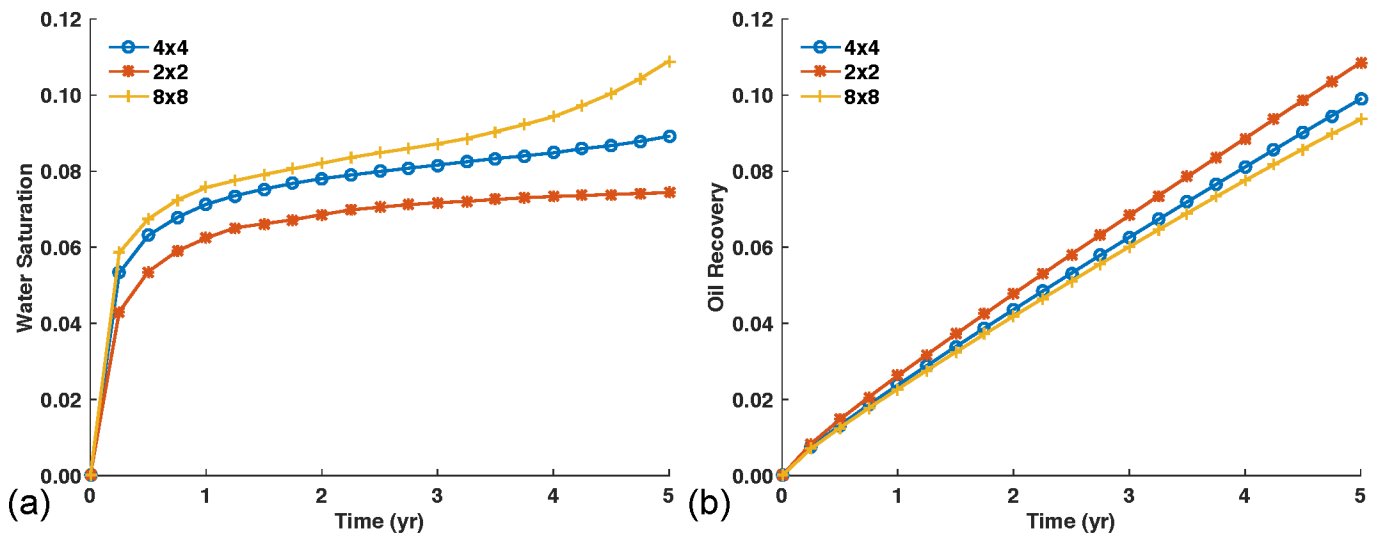


Figure 7: Water saturation in the production well (a) and oil recovery (b) for simulations in which the matrix block size is varied from the base-case of $4 \times 4 \text{ m}^2$ to $2 \times 2 \text{ m}^2$ and $8 \times 8 \text{ m}^2$. Domain size is $52 \times 200 \text{ m}^2$.

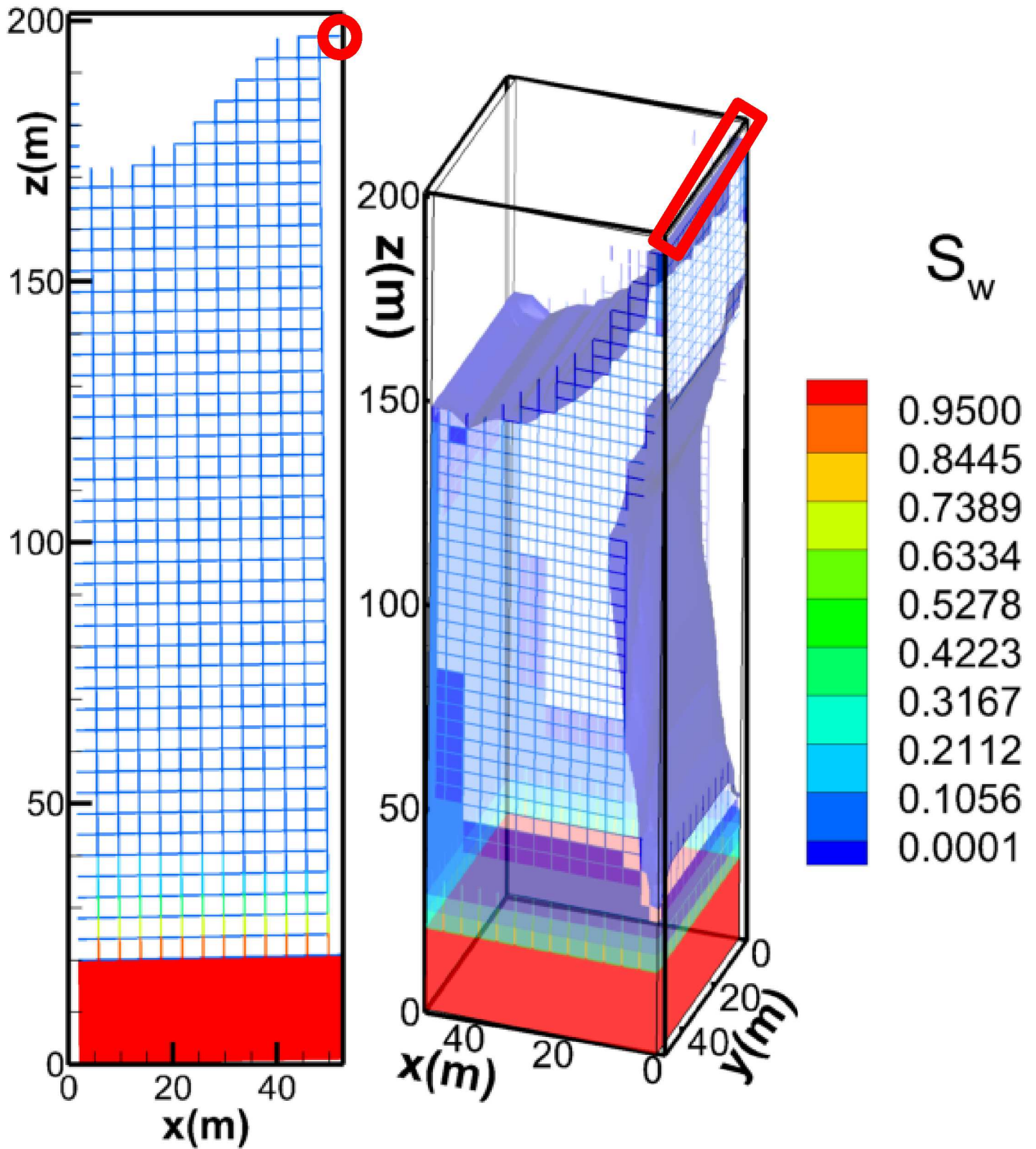


Figure 8: Water saturation at $t = 6$ months for 2D and 3D simulations on $52 \times 200 \text{ m}^2$ and $52 \times 52 \times 200 \text{ m}^3$ domains, respectively.

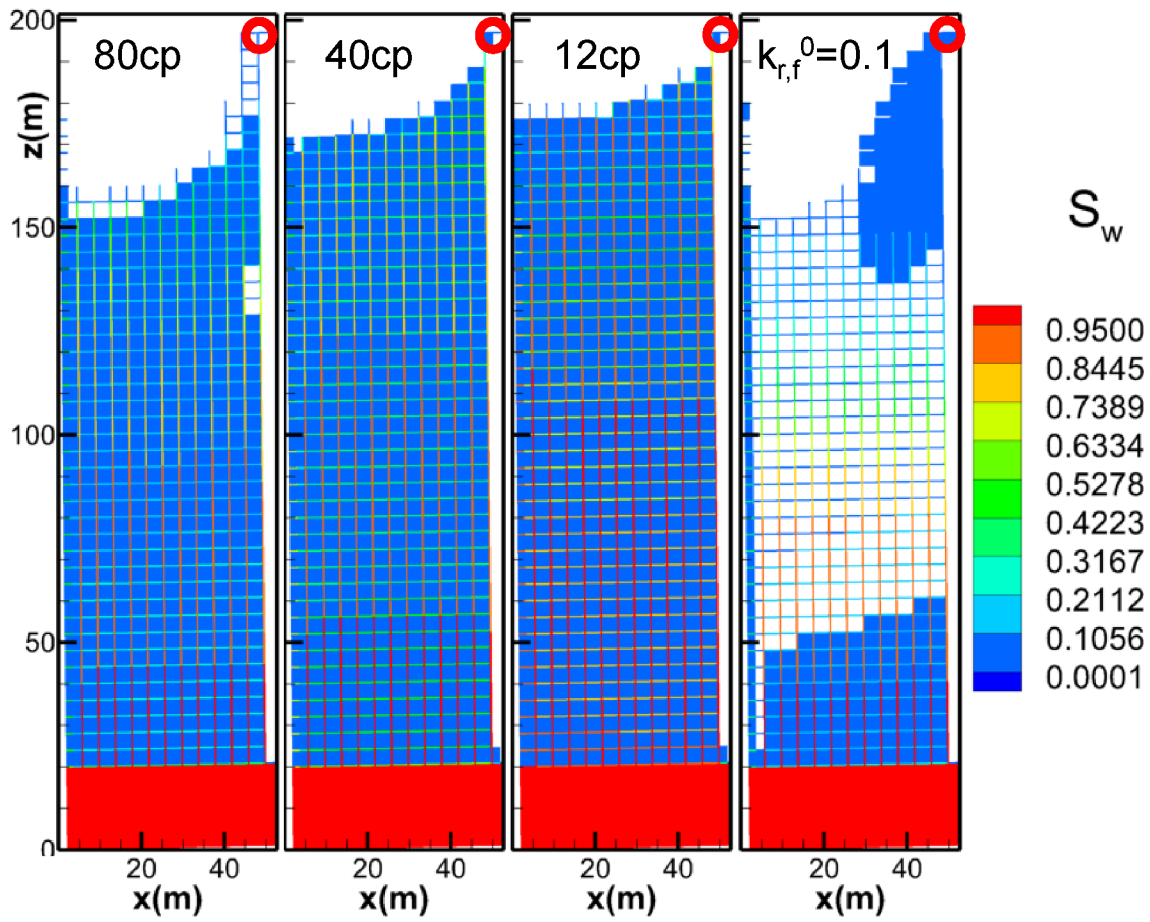


Figure 9: Water saturation at $t = 5$ years for simulations in which oil viscosities are reduced from the base-case of 121 cp to 80, 40, and 12 cp, as well as a simulation for an end-point relative permeability of $k_{r,f}^0 = 0.1$ for water in the fractures. Domain size is $52 \times 200 \text{ m}^2$.

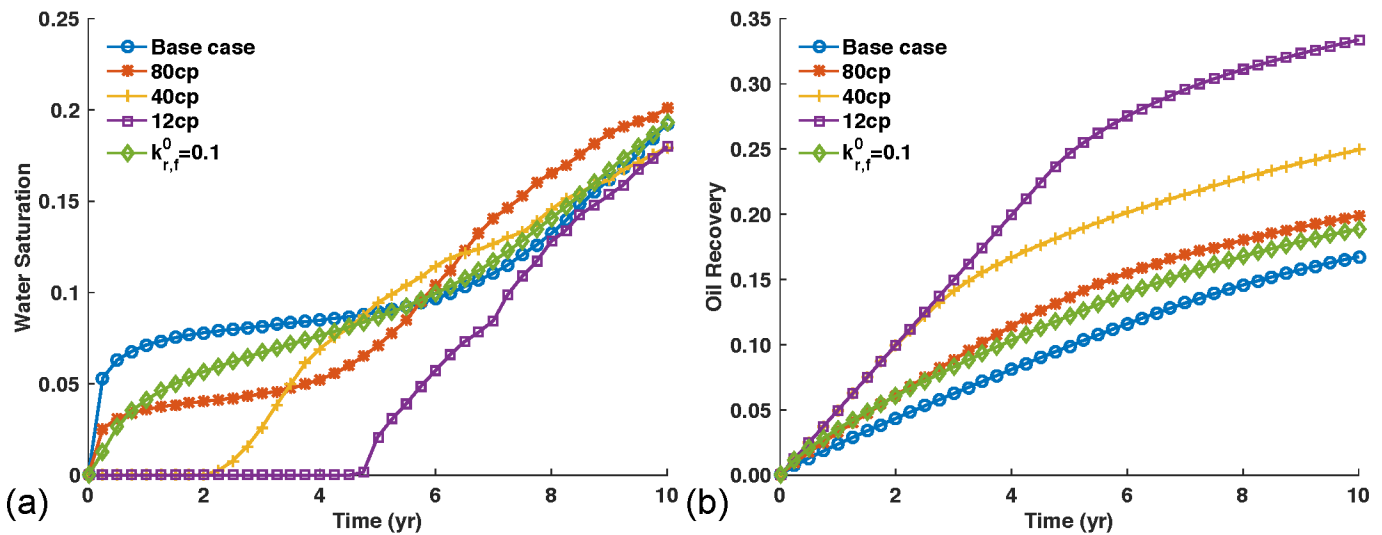


Figure 10: Water saturation in the production well (a) and oil recovery (b) for simulations in which oil viscosities are reduced from the base-case of $\mu_o = 121$ cp to 80, 40, and 12 cp, as well as a simulation for an end-point relative permeability of $k_{r,f}^0 = 0.1$ for water in the fractures.

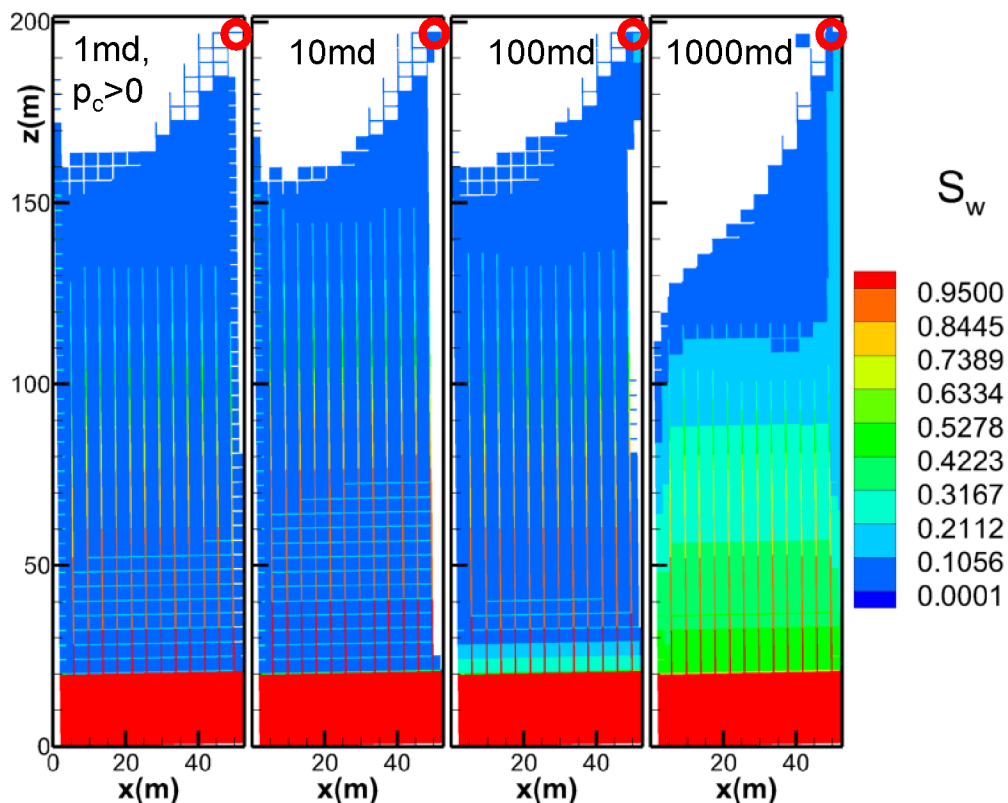


Figure 11: Water saturation at $t = 5$ years for a simulation with the capillary pressure from Figure 1 (left) and for simulations in which the matrix permeability is varied from the base-case of 1 md to larger 10, 100, and 1000 md permeabilities. Domain size is $52 \times 200 \text{ m}^2$.

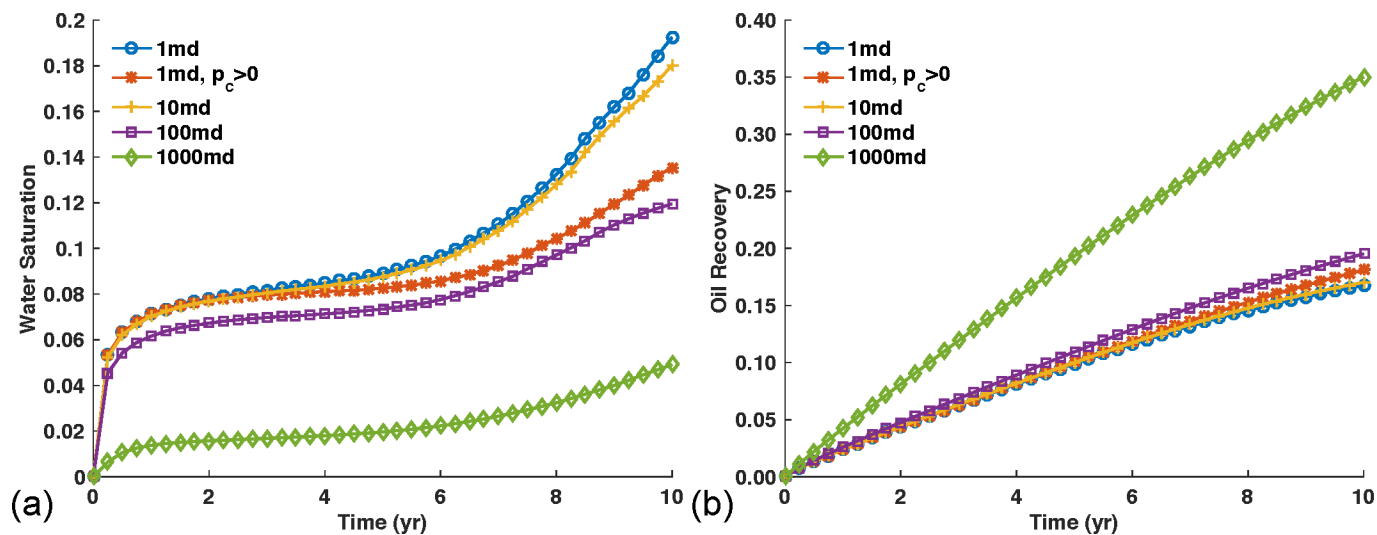


Figure 12: Water saturation in the production well (a) and oil recovery (b) for a simulation with the capillary pressure from Figure 1 (left) and for simulations in which the matrix permeability is varied from the base-case of 1 md to larger 10, 100, and 1000 md permeabilities.

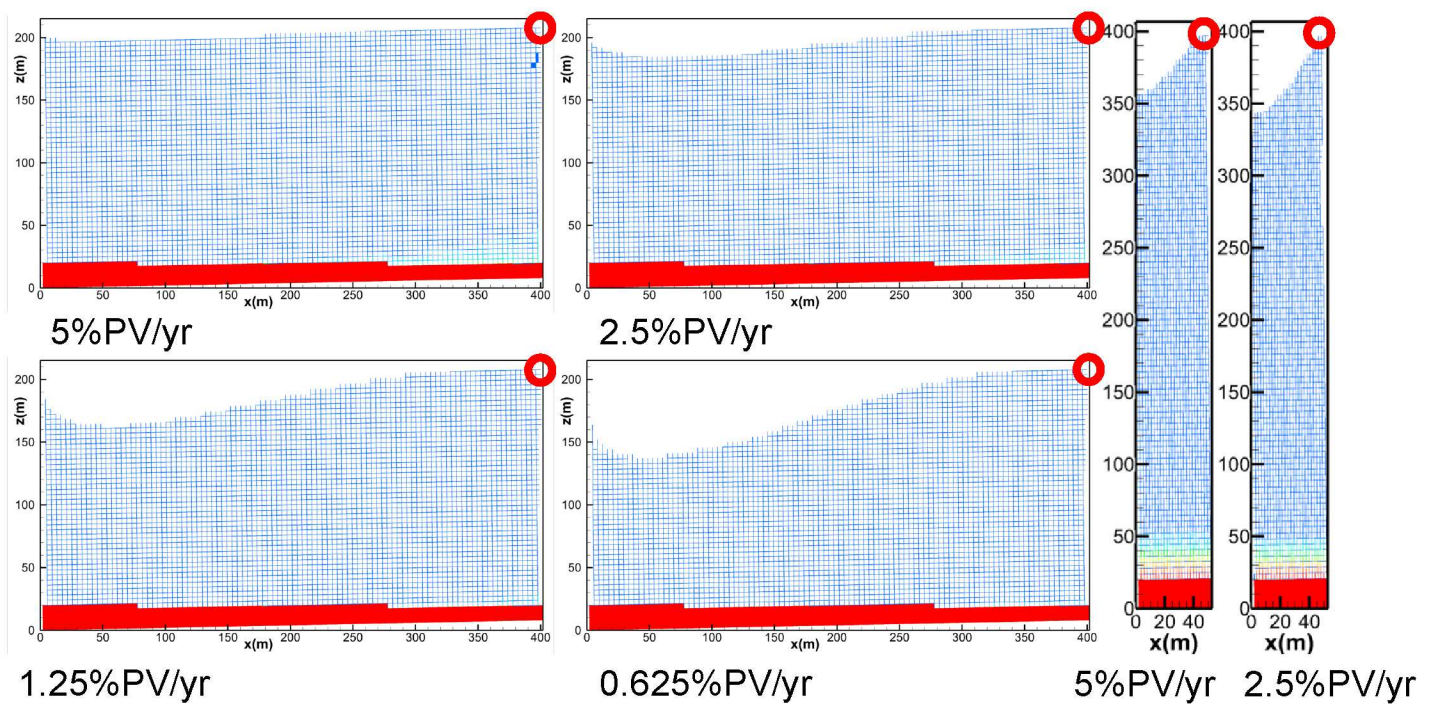


Figure 13: Water saturation at $t = 1$ years for simulations in which the domain size is varied from the base-case of $52 \times 200 \text{ m}^2$ to a much wider domain of $400 \times 200 \text{ m}^2$ or a much thicker domain of $52 \times 400 \text{ m}^2$. Injection rates of 0.625, 1.25, 2.5, and 5% PV/yr are modeled for the former and rates of 2.5 and 5% PV/yr for the latter.

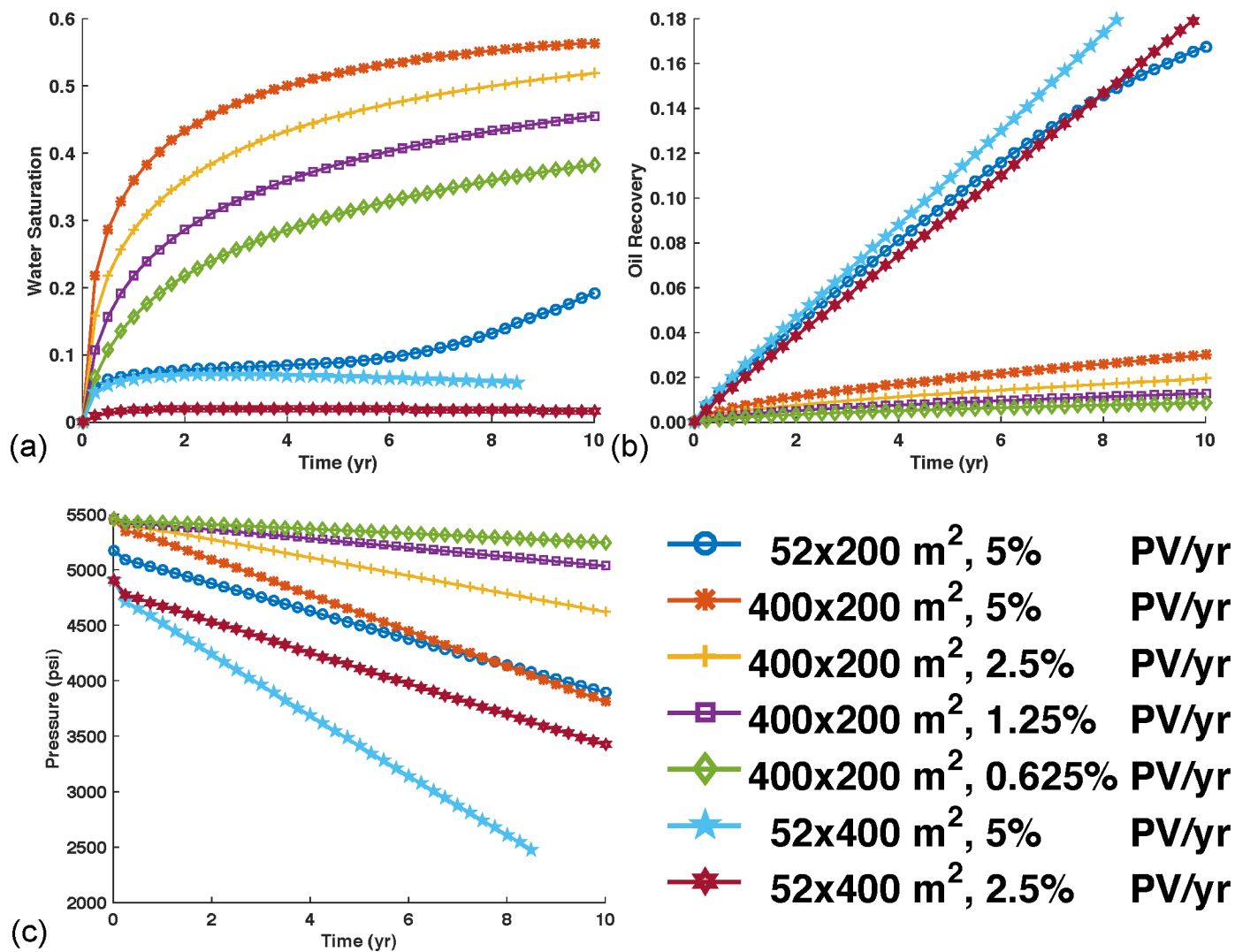


Figure 14: Water saturation in the production well (a), oil recovery (b), and pressure in production well (c) for simulations in which the domain size is varied from the base-case of $52 \times 200 \text{ m}^2$ to a much wider domain of $400 \times 200 \text{ m}^2$ or a much thicker domain of $52 \times 400 \text{ m}^2$. Injection rates of 0.625, 1.25, 2.5, and 5% PV/yr are modeled for the former and rates of 2.5 and 5% PV/yr for the latter.

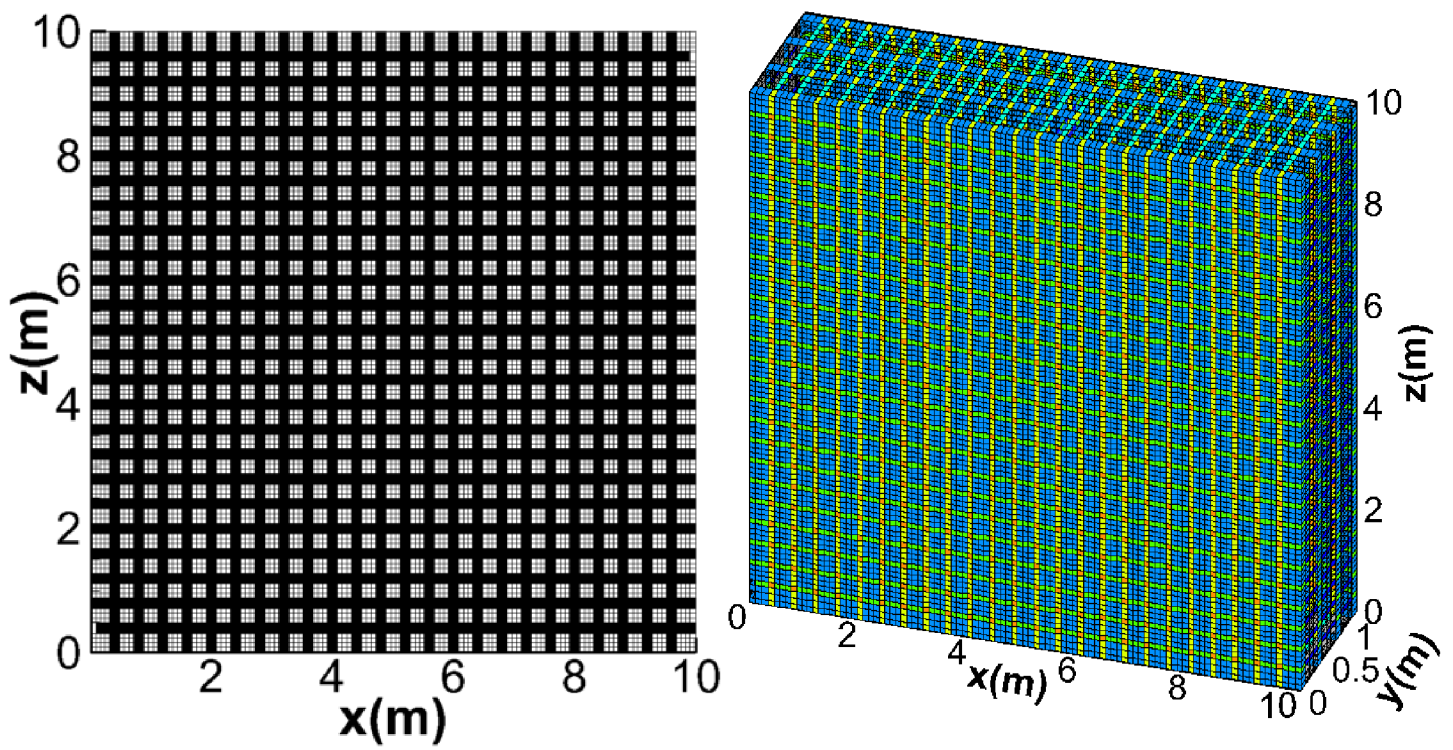


Figure 15: 99×99 element 2D mesh and $99 \times 13 \times 99$ element 3D mesh (Grid 2) and with matrix blocks of 40 cm in each direction surrounded by fractures (and vugs).

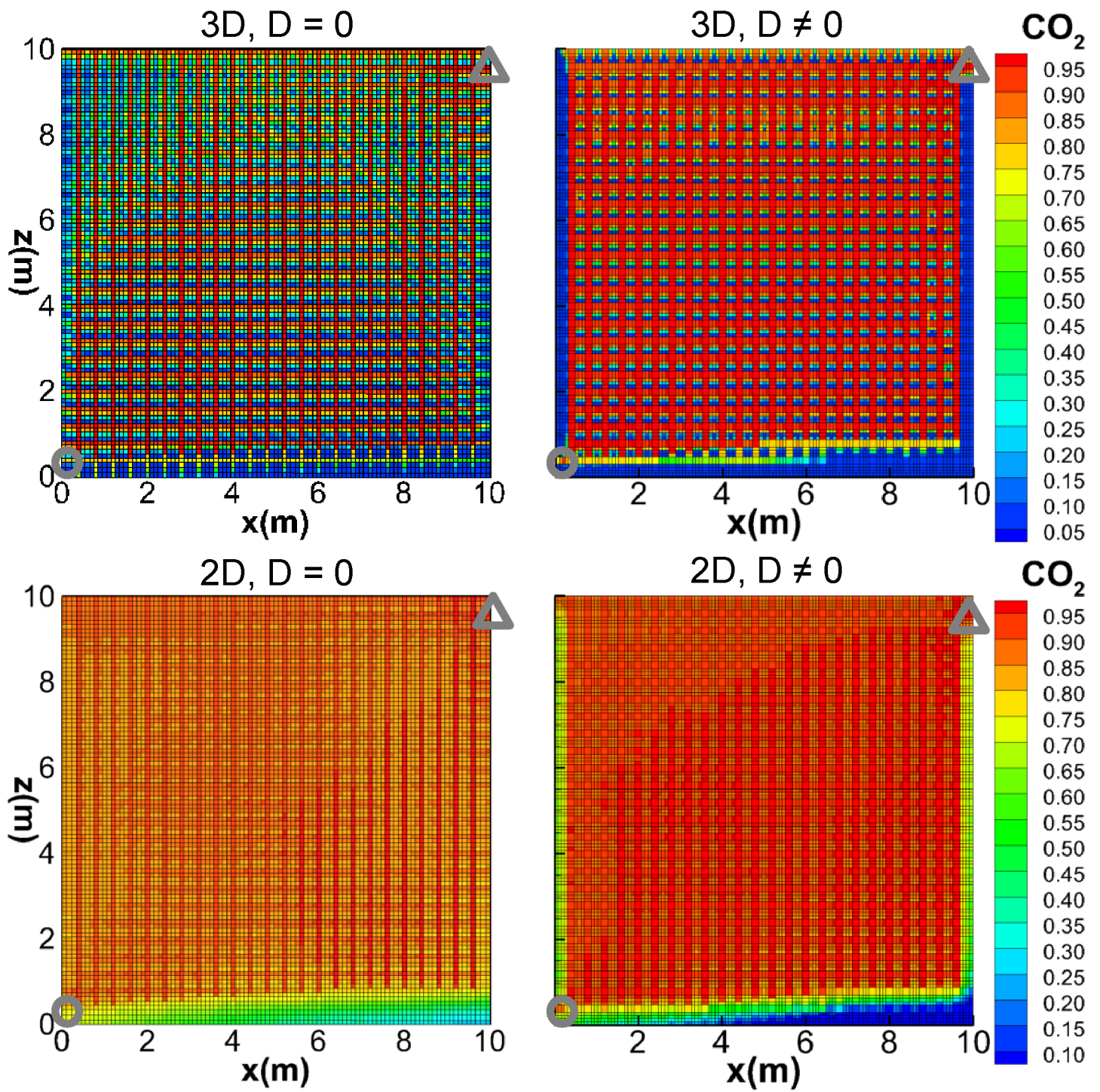


Figure 16: CO₂ molar fraction for 2D simulations and for a cross-section at $y = 0.6$ m of 3D simulations without ($D = 0$) and with ($D \neq 0$) Fickian diffusion. Injection well is indicated by a triangle, production well by a circle.

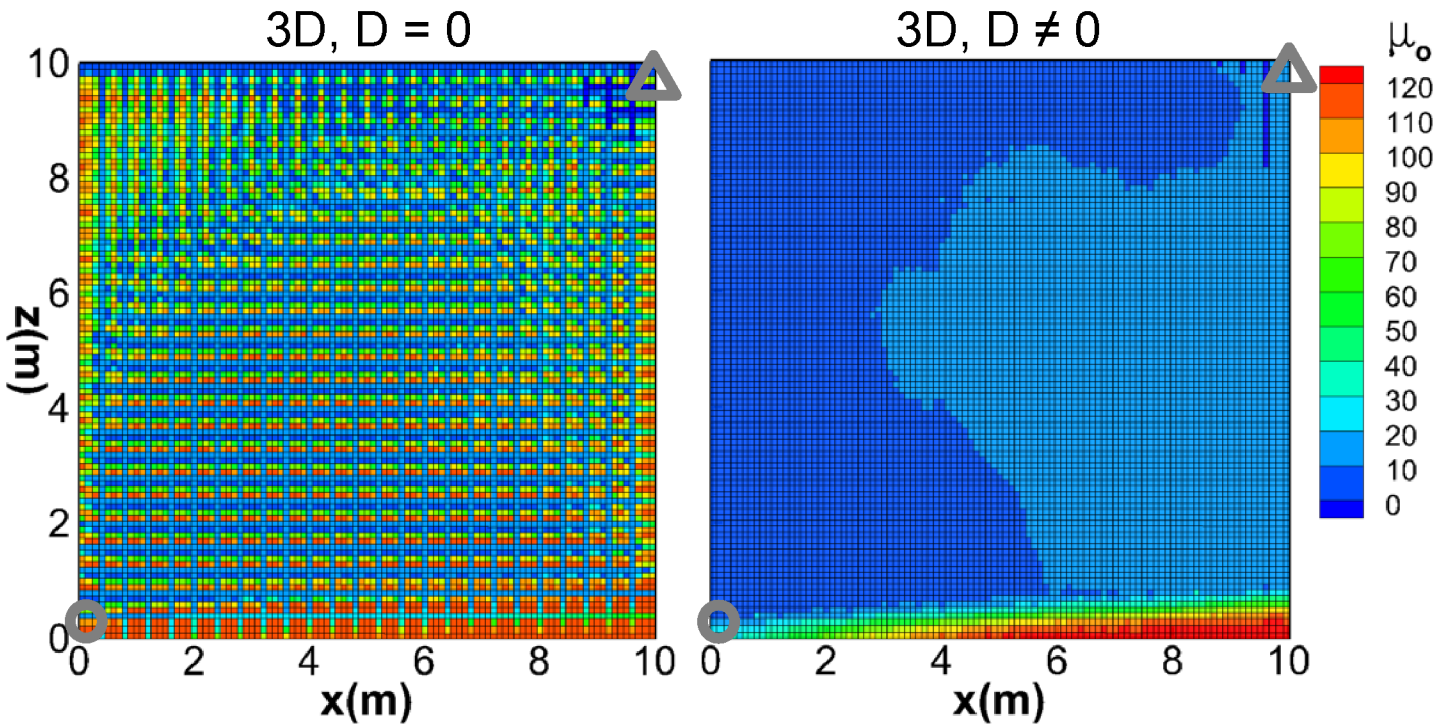


Figure 17: Oil viscosity (cp) for a cross-section at $y = 0.6$ m of 3D simulations without ($D = 0$) and with ($D \neq 0$) Fickian diffusion. Injection well is indicated by a triangle, production well by a circle.

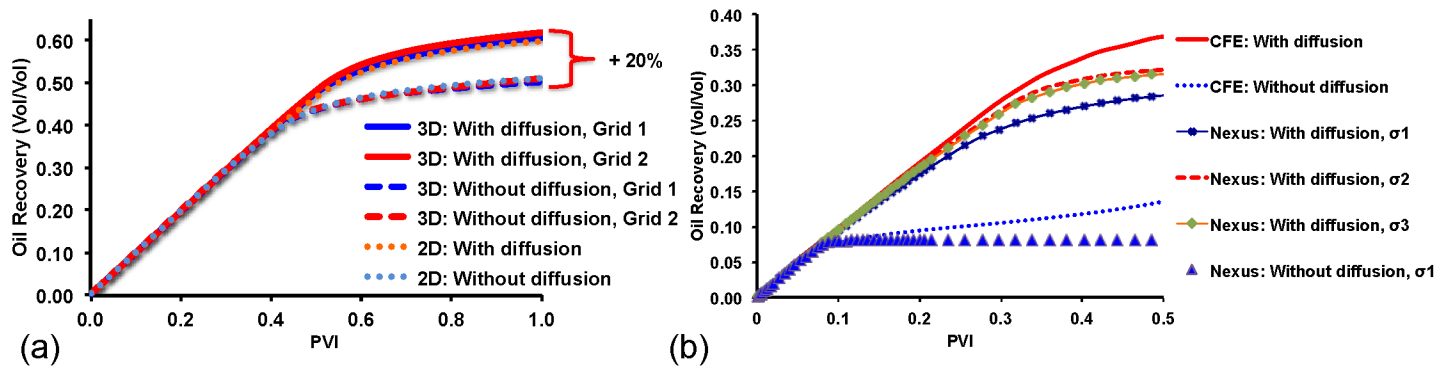


Figure 18: Oil recoveries for CO_2 injection in 2D and 3D densely fractured domains with and without Fickian diffusion (a) and a comparison between our CFE model and the dual-porosity Nexus reservoir simulator with 3 different shape factors defined in Equation 1.

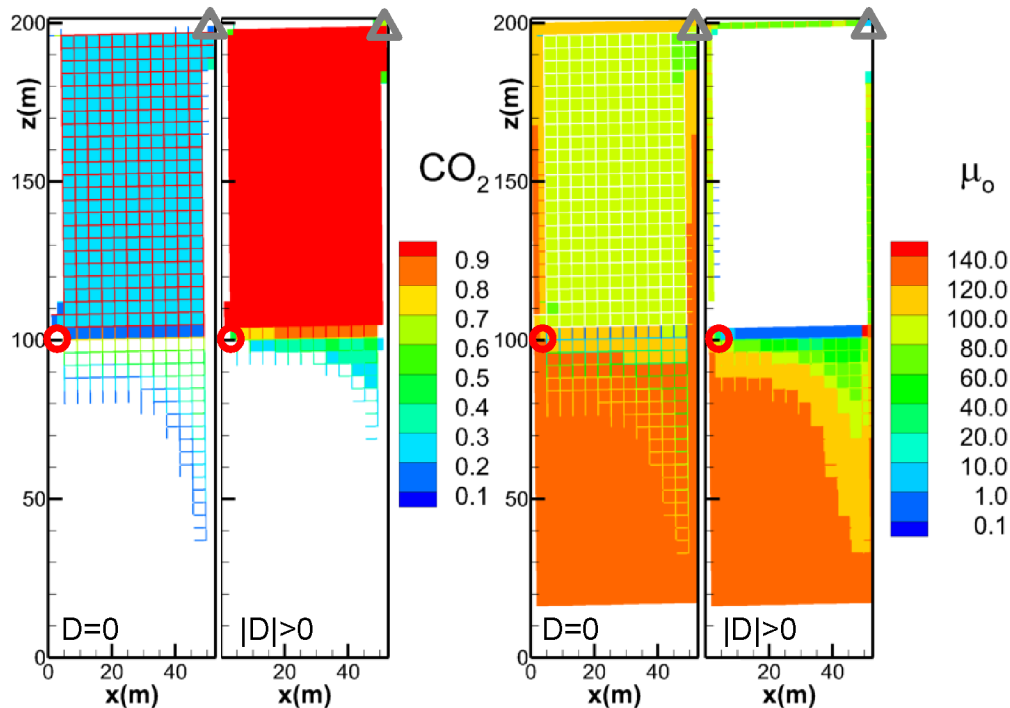


Figure 19: CO₂ molar fraction (left) and oil viscosity (right) for simulations of CO₂ injection at 2.5% PV/yr without and with diffusion in the same grid as in Figure 4.

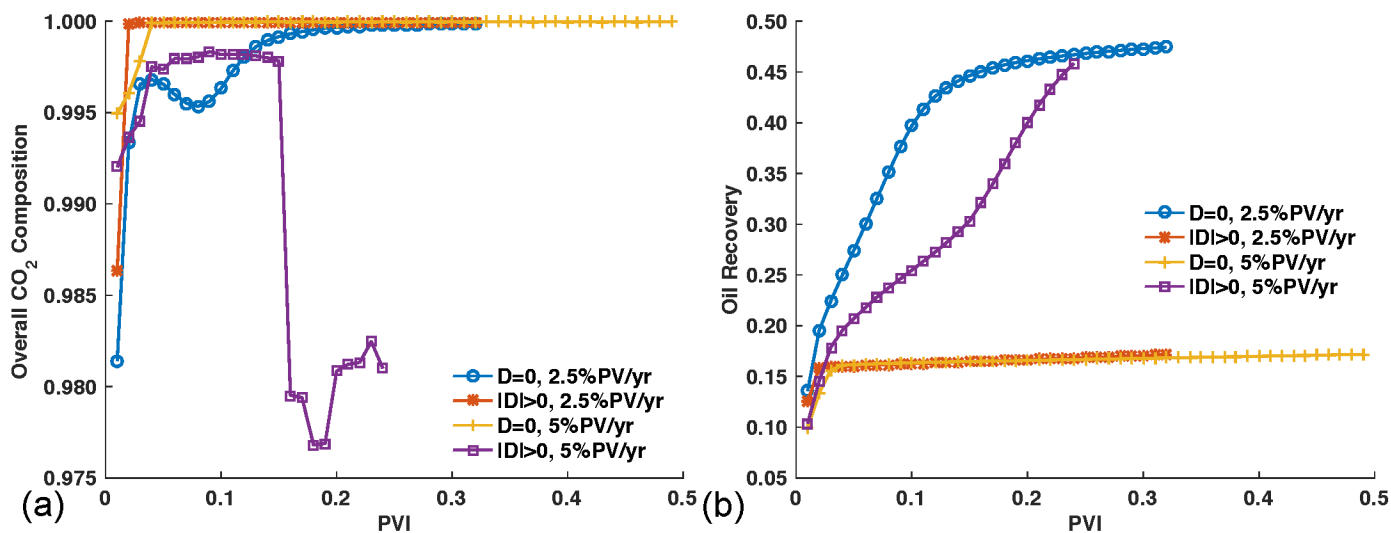


Figure 20: CO₂ molar fraction in the production well (a) and oil recovery (b) for simulations of CO₂ injection without and with diffusion on the same grid as in Figure 4.